Geochemical Studies of Rare Earth Elements in the Portuguese Pyrite Belt, and Geologic and Geochemical Controls on Gold Distribution

Edited by David J. Grimes *and* S.J. Kropschot

A. Rare Earth Element Distribution in the Volcanic Lithostratigraphic Units of the Portuguese Pyrite Belt
By David J. Grimes, Robert L. Earhart, *and* Delfim de Carvalho

B. Geologic Setting and Geochemical Controls on the Distribution of Gold in the Portuguese Pyrite Belt
By Robert L. Earhart, Delfim de Carvalho, Vitor Oliveira, Jose T. Oliveira, *and* Paulo Castro

---

U.S. GEOLOGICAL SURVEY PROFESSIONAL PAPER 1596–A–B

Prepared in cooperation with the
Luso American Development Foundation, the
Serviços Geológicos de Portugal, and the Serviço
de Fomento Mineiro

UNITED STATES GOVERNMENT PRINTING OFFICE, WASHINGTON : 1998

U.S. DEPARTMENT OF THE INTERIOR

BRUCE BABBITT, Secretary

U.S. GEOLOGICAL SURVEY

Thomas J. Casadevall, Acting Director

For sale by U.S. Geological Survey, Information Services
Box 25286, Federal Center
Denver, CO 80225

Library of Congress Cataloging-in-Publication Data

Geochemical studies of rare earth elements in the Portuguese Pyrite Belt, and geologic and geochemical controls on gold distribution / edited by David J. Grimes and S. J. Kropschot.

p. cm.—(U.S. Geoloigcal Survey professional paper ; 1596)

"Prepared with the support and cooperation of the Luso American Development Foundation, the Serviços Geológicos de Portugal, and the Serviços de Fomento Mineiro."

Includes bibliographical references.

Contents: Rare earth element distribution in the volcanic lithostratigraphic units of the Portuguese Pyrite Belt / by David J. Grimes, Robert L. Earhart, and Delfim de Carvalho — Geologic setting and geochemical controls on the distribution of gold in the Portuguese Pyrite Belt / by Robert L. Earhart . . . [et al.].

1. Geochemistry—Portugal. 2. Rare earth metals—Portugal. 3. Gold ores—Portugal. I. Grimes, D. J. (David J.), 1943–. II. Kropschot, S. J. (Susan J.) III. Luso-American Development Foundation. IV. Serviços Geológicos de Portugal. V. Portugal, Serviços de Fomento Mineiro. VI. Series.

QE516.R2G435 1998
[553.4′94′09469—dc21 98—10121
CIP

AVAILABILITY OF BOOKS AND MAPS OF THE U.S. GEOLOGICAL SURVEY

Instructions on ordering publications of the U.S. Geological Survey, along with prices of the last offerings, are given in the current-year issues of the monthly catalog “New Publications of the U.S. Geological Survey.” Prices of available U.S. Geological Survey publications released prior to the current year are listed in the most recent annual “Price and Availability List.” Publications that may be listed in various U.S. Geological Survey catalogs (**see back inside cover**) but not listed in the most recent annual “Price and Availability List” may no longer be available.

Reports released through the NTIS may be obtained by writing to the National Technical Information Service, U.S. Department of Commerce, Springfield, VA 22161; please include NTIS report number with inquiry.

Order U.S. Geological Survey publications **by mail** or **over the counter** from the offices listed below.

BY MAIL

Books

Professional Papers, Bulletins, Water-Supply Papers, Techniques of Water-Resources Investigations, Circulars, publications of general interest (such as leaflets, pamphlets, booklets), single copies of Earthquakes & Volcanoes, Preliminary Determination of Epicenters, and some miscellaneous reports, including some of the foregoing series that have gone out of print at the Superintendent of Documents, are obtainable by mail from

U.S. Geological Survey, Map Distribution
Box 25286, MS 306, Federal Center
Denver, CO 80225

Subscriptions to periodicals (Earthquakes & Volcanoes and Preliminary Determination of Epicenters) can be obtained ONLY from the

Superintendent of Documents
Government Printing Office
Washington, DC 20402

(Check or money order must be payable to Superintendent of Documents.)

Maps

For maps, address mail orders to

U. S. Geological Survey, Map Distribution
Box 25286, Bldg. 810, Federal Center
Denver, CO 80225

Residents of Alaska may order maps from

U.S. Geological Survey, Earth Science Information Center
4230 University Dr., Rm. 101
Anchorage, AK 99508–4664

OVER THE COUNTER

Books and Maps

Books and maps of the U.S. Geological Survey are available over the counter at the following U.S. Geological Survey offices, all of which are authorized agents of the Superintendent of Documents.

- **ANCHORAGE, Alaska**–Rm. 101, 4230 University Dr.
- **LAKEWOOD, Colorado**–Federal Center, Bldg. 810
- **MENLO PARK, California**–Bldg. 3, Rm. 3128, 345 Middlefield Rd.
- **RESTON, Virginia**–USGS National Center, Rm. 1C402, 12201 Sunrise Valley Dr.
- **SALT LAKE CITY, Utah**–Federal Bldg., Rm. 8105, 125 South State St.
- **SPOKANE, Washington**–U.S. Post Office Bldg., Rm. 135, West 904 Riverside Ave.
- **WASHINGTON, D.C**.–Main Interior Bldg., Rm. 2650, 18th and C Sts., NW.

Maps Only

Maps may be purchased over the counter at the following U.S. Geological Survey offices:

- **ROLLA, Missouri**–1400 Independence Rd.

SELECTED SERIES OF U.S. GEOLOGICAL SURVEY PUBLICATIONS

Periodicals

Earthquakes & Volcanoes (issued bimonthly).
Preliminary Determination of Epicenters (issued monthly).

Technical Books and Reports

Professional Papers are mainly comprehensive scientific reports of wide and lasting interest and importance to professional scientists and engineers. Included are reports on the results of resource studies and of topographic, hydrologic, and geologic investigations. They also include collections of related papers addressing different aspects of a single scientific topic.

Bulletins contain significant data and interpretations that are of lasting scientific interest but are generally more limited in scope or geographic coverage than Professional Papers. They include the results of resource studies and of geologic and topographic investigations; as well as collections of short papers related to a specific topic.

Water-Supply Papers are comprehensive reports that present significant interpretive results of hydrologic investigations of wide interest to professional geologists, hydrologists, and engineers. The series covers investigations in all phases of hydrology, including hydrology, availability of water, quality of water, and use of water.

Circulars present administrative information or important scientific information of wide popular interest in a format designed for distribution at no cost to the public. Information is usually of short-term interest.

Water-Resources Investigations Reports are papers of an interpretive nature made available to the public outside the formal USGS publications series. Copies are reproduced on request unlike formal USGS publications, and they are also available for public inspection at depositories indicated in USGS catalogs.

Open-File Reports include unpublished manuscript reports, maps, and other material that are made available for public consultation at depositories. They are a nonpermanent form of publication that may be cited in other publications as sources of information.

Maps

Geologic Quadrangle Maps are multicolor geologic maps on topographic bases in 7 1/2- or 15-minute quadrangle formats (scales mainly 1:24,000 or 1:62,500) showing bedrock, surficial, or engineering geology. Maps generally include brief texts; some maps include structure and columnar sections only.

Geophysical Investigations Maps are on topographic or planimetric bases at various scales, they show results of surveys using geophysical techniques, such as gravity, magnetic, seismic, or radioactivity, which reflect subsurface structures that are of economic or geologic significance. Many maps include correlations with the geology.

Miscellaneous Investigations Series Maps are on planimetric or topographic bases of regular and irregular areas at various scales; they present a wide variety of format and subject matter. The series also includes 7 1/2-minute quadrangle photogeologic maps on planimetric bases which show geology as interpreted from aerial photographs. The series also includes maps of Mars and the Moon.

Coal Investigations Maps are geologic maps on topographic or planimetric bases at various scales showing bedrock or surficial geology, stratigraphy, and structural relations in certain coal-resource areas.

Oil and Gas Investigations Charts show stratigraphic information for certain oil and gas fields and other areas having petroleum potential.

Miscellaneous Field Studies Maps are multicolor or black-and-white maps on topographic or planimetric bases on quadrangle or irregular areas at various scales. Pre-1971 maps show bedrock geology in relation to specific mining or mineral-deposit problems; post-1971 maps are primarily black-and-white maps on various subjects such as environmental studies or wilderness mineral investigations.

Hydrologic Investigations Atlases are multicolored or black-and-white maps on topographic or planimetric bases presenting a wide range of geohydrologic data of both regular and irregular areas; the principal scale is 1:24,000, and regional studies are at 1:250,000 scale or smaller.

Catalogs

Permanent catalogs, as well as some others, giving comprehensive listings of U.S. Geological Survey publications are available under the conditions indicated below from USGS Map Distribution, Box 25286, Building 810, Denver Federal Center, Denver, CO 80225. (See latest Price and Availability List.)

"Publications of the Geological Survey, 1879-1961" may be purchased by mail and over the counter in paperback book form and as a set microfiche.

"Publications of the Geological Survey, 1962-1970" may be purchased by mail and over the counter in paperback book form and as a set of microfiche.

"Publications of the U.S. Geological Survey, 1971-1981" may be purchased by mail and over the counter in paperback book form (two volumes, publications listing and index) and as a set of microfiche.

Supplements for 1982, 1983, 1984, 1985, 1986, and for subsequent years since the last permanent catalog may be purchased by mail and over the counter in paperback book form.

State catalogs, "List of U.S. Geological Survey Geologic and Water-Supply Reports and Maps For (State)," may be purchased by mail and over the counter in paperback booklet form only.

"Price and Availability List of U.S. Geological Survey Publications," issued annually, is available free of charge in paperback booklet form only.

Selected copies of a monthly catalog "New Publications of the U.S. Geological Survey" is available free of charge by mail or may be obtained over the counter in paperback booklet form only. Those wishing a free subscription to the monthly catalog "New Publications of the U.S. Geological Survey" should write to the U.S. Geological Survey, 582 National Center, Reston, VA 22092.

Note.–Prices of Government publications listed in older catalogs, announcements, and publications may be incorrect. Therefore, the prices charged may differ from the prices in catalogs, announcements, and publications.

CONTENTS

PLATES

[Plates are in pocket]

FIGURES

TABLES

GEOCHEMICAL STUDIES OF RARE EARTH ELEMENTS IN THE PORTUGUESE PYRITE BELT, AND GEOLOGIC AND GEOCHEMICAL CONTROLS ON GOLD DISTRIBUTION

ABSTRACT

Geochemical and geologic studies were conducted by the U.S. Geological Survey and the Serviços Geológicos de Portugal in the Portuguese Pyrite Belt in southern Portugal during 1987 and 1988. Under a cooperative agreement, the Serviços Geológicos de Portugal provided logistical support and background information needed to carry out the investigations as well as technical assistance in one of the study areas. Principal funding was provided by the Luso American Development Foundation, supplemented by the U.S. Geological Survey and the Serviços Geológicos de Portugal.

The studies included (1) rare earth element distributions, (2) testing and development of geochemical methods, and (3) identification of geologic and geochemical controls on the distribution of gold. Reconnaissance and detailed geologic studies were conducted and rock, soil, plant, and water samples were collected for chemical analyses as part of the geochemical surveys.

The Portuguese Pyrite Belt is the part of the Iberian Pyrite Belt that trends eastward from near Seville in southern Spain across southern Portugal. The Iberian Pyrite Belt is about 230 km long and 30 km wide and the geology is structurally complex, consisting of Late Paleozoic volcanic and sedimentary rocks. The Iberian Pyrite Belt is host to numerous copper-, zinc-, and lead-bearing massive sulfide deposits and contains the largest reserve of metals in Western Europe. The massive sulfide deposits are hosted in Late Devonian to Early Carboniferous felsic volcanic and sedimentary rocks.

Rare earth element distributions were determined in representative samples of volcanic rocks from five west-trending sub-belts of the Portuguese Pyrite Belt to test the usefulness of rare earth element distributions to correlate volcanic events, and to examine if their mobility has any application as hydrothermal tracers. Rare earth element distributions in felsic volcanic rocks show decreases in the relative abundances of heavy rare earth elements and an increase in La/Yb ratios from south to north in the Portuguese Pyrite Belt. Basalt in one of the sub-belts shows relative enrichment in light rare earth elements with respect to the other sub-belts. More rare earth element analyses are needed to provide definitive data that may be used in the correlation of volcanic events. Variations in the distribution of rare earth elements in felsic volcanic rocks in the Neves-Corvo area reflect type and intensity of alteration. Altered felsic volcanic rocks that host massive sulfide deposits contain pronounced negative europium anomalies. These data may be useful geochemical indicators in the selection of targets for buried massive sulfide deposits.

Anomalous amounts of gold are distributed in and near massive and disseminated sulfide deposits in the Portuguese Pyrite Belt. Gold is closely associated with copper in the middle and lower parts of the deposits. In the exhalative sedimentary rocks that are stratigraphically above massive sulfide deposits, weakly anomalous concentrations of gold were detected in a distal manganiferous facies and anomalously low concentrations of gold were detected in the barite-rich, proximal-facies exhalites. In contrast, two samples collected from the proximal facies pyritiferous cherts at São Domingos in the northeastern part of the Portuguese Pyrite Belt, contained high concentrations of gold; here, Ag, As, Bi, Mo, Pb, and Sb, are associated with gold.

Altered and pyritic felsic volcanic rocks locally contain highly anomalous concentrations of gold, suggesting that the potential for gold in disseminated sulfide deposits and the nonore-bearing parts of massive sulfide deposits should be evaluated. The São Domingos, Chança, and Salgadinho sulfide deposits, and adjacent rocks are particularly favorable areas for gold exploration; arsenic and molybdenum are commonly associated with the gold. Additional pathfinder elements include silver, copper, antimony, and lead. The felsic volcanic rocks of the Portuguese Pyrite Belt are hydrothermally altered. Sericite occurs as an alteration product over large areas and is locally associated with gold. Most samples, however, contain very low concentrations of gold. Anomalous gold was detected primarily in highly silicified and pyritized rock samples. Silicified and pyritized rocks should routinely be tested for gold, particularly where they are highly fractured and where they overlie or are lateral to disseminated or massive sulfide deposits.

Serpentinite and altered serpentinite (listwaenite) rock samples from the Ossa-Morena zone adjacent to the Iberian Pyrite Belt were tested for gold and were found to contain below average abundances; extensive quartz veins that are characteristic of gold deposits in some ultramafic rock terranes appear to be lacking.

INTRODUCTION

Geologic and geochemical studies in the Portuguese part of the Iberian Pyrite Belt were conducted during a cooperative program funded by the Luso American Development Foundation (LADF). Supplemental funding was provided by the Serviços Geológicos de Portugal and by the U.S. Geological Survey. The project was initiated in November 1986 and field work was conducted in the summers of 1987 and 1988. Samples were analyzed in the laboratories of the USGS in Denver, Colorado.

The Iberian Pyrite Belt (IPB) covers an area about 230 km long and 30 km wide (fig. 1). The IPB is the largest metallogenic province in Western Europe and a major producer of iron pyrite, copper, and zinc. Approximately half of the IPB is in southern Portugal and in this paper is referred to as the Portuguese Pyrite Belt (PPB) (fig. 2). The Neves-Corvo deposit in Portugal contains large reserves of tin and is the largest source of tin in Western Europe. All of the deposits in the PPB are classified as volcanogenic massive sulfide deposits and are hosted by submarine felsic volcanic rocks of Late Paleozoic age.

The purpose of the present cooperative studies are to develop of methods applicable to the exploration for additional metallic mineral deposits in the metallogenic province. The objectives of the program, as stated in 1987, are as follows: (1) Through the study of the rare earth element (REE) distributions in volcanic and volcanic-sedimentary lithostratigraphic units of the Portuguese Pyrite Belt, contribute to a better understanding of ore-forming processes and of post-mineral modifications in the massive sulfide environment. Results of the current study are reported in chapter A. (2) Using the above information, the results of detailed stratigraphic studies of the volcanic and volcanic-sedimentary rocks, and the results of geochemical exploration investigations, develop effective exploration methods applicable to the PPB and similar geologic terranes. Results are reported in Grimes and Carvalho (1995). (3) Determine the lithostratigraphic and geochemical controls on the distribution of gold in the PPB. Results of the current study are reported in chapter B.

INVESTIGATIVE METHODS AND CONSIDERATIONS

Geologic and geochemical investigations were conducted over widely scattered localities in the PPB. Previous studies in the PPB provided the background for the current studies. Those that were particularly applicable include investigations by Carvalho, (1974, 1976, 1979, 1991), Leca and others (1983), Munhá (1983), Oliveira (1983), Plimer and Carvalho (1982), and Schermerhorn (1970, 1971).

Samples of felsic and mafic volcanic rocks were collected from the five volcanic sub-belts (A-E) shown in figure 2 as part of the REE study. Particular emphasis was placed on the felsic rocks. In areas where more than one felsic volcanic unit could be identified, samples were collected from each unit. Samples were also collected from three felsic units exposed in the underground workings at Neves-Corvo near the massive sulfide deposits to compare the REE chemistry of samples from mineralized and altered localities with those from unmineralized and unaltered localities. These comparisons are useful in determining REE mobility associated with hydrothermal events in the PPB. As part of the development of new exploration techniques, samples of rocks, soils, plants, and ground water were collected at various localities in the PPB. The results of this study are reported by Grimes and Carvalho (1995) and will not be discussed here.

In order to determine the lithostratigraphic and geochemical controls on the distribution of gold, geologic and geochemical baseline data were collected in the PPB and in similar geologic environments. Gold in massive sulfide deposits in other parts of the world is well documented (Huston and Large, 1989). In the IPB, gold has been recovered from some pyrite and base metal mines and from the near-surface oxidized parts of massive sulfide deposits.

Attention is primarily focused on geologic subenvironments other than the massive sulfide deposits in this study. Prior to the present investigations, gold and associated element distributions beyond the limits of the massive sulfide deposits were poorly known and not recognized as potential environments for gold. An interim project report on the distribution of gold and associated elements in cherts (exhalites) was submitted to Luso American Development Foundation (Serviços Geológicos de Portugal and U.S.Geological Survey, 1988).

Identification of favorable subenvironments for gold deposits, other than massive sulfide deposits, in the PPB and in the South Portuguese Zone (the tectonic province that hosts the PPB) is made on the basis on modern studies of gold deposits. The geologic subenvironments in the PPB can be compared with similar geologic terranes or lithostratigraphic provinces in other parts of the world where gold deposits are found. In the PPB these subenvironments include chert terranes (exhalites), hangingwall rocks of massive sulfide deposits (São Domingos), and siliceous and tuffaceous volcanic-sedimentary rocks with disseminated sulfides (Salgadinho).

GEOLOGIC SETTING

The PPB is a part of the IPB that trends westward to northwestward through southern Portugal. The IPB extends into Spain and is about 230 km long and ranges from 30 to 50 km wide (fig. 1). The IPB contains numerous volcanogenic massive sulfide deposits and is the largest mining belt with the largest reserves of metals in Western Europe. Ore reserves in the IPB are about equally divided between Portugal and Spain.

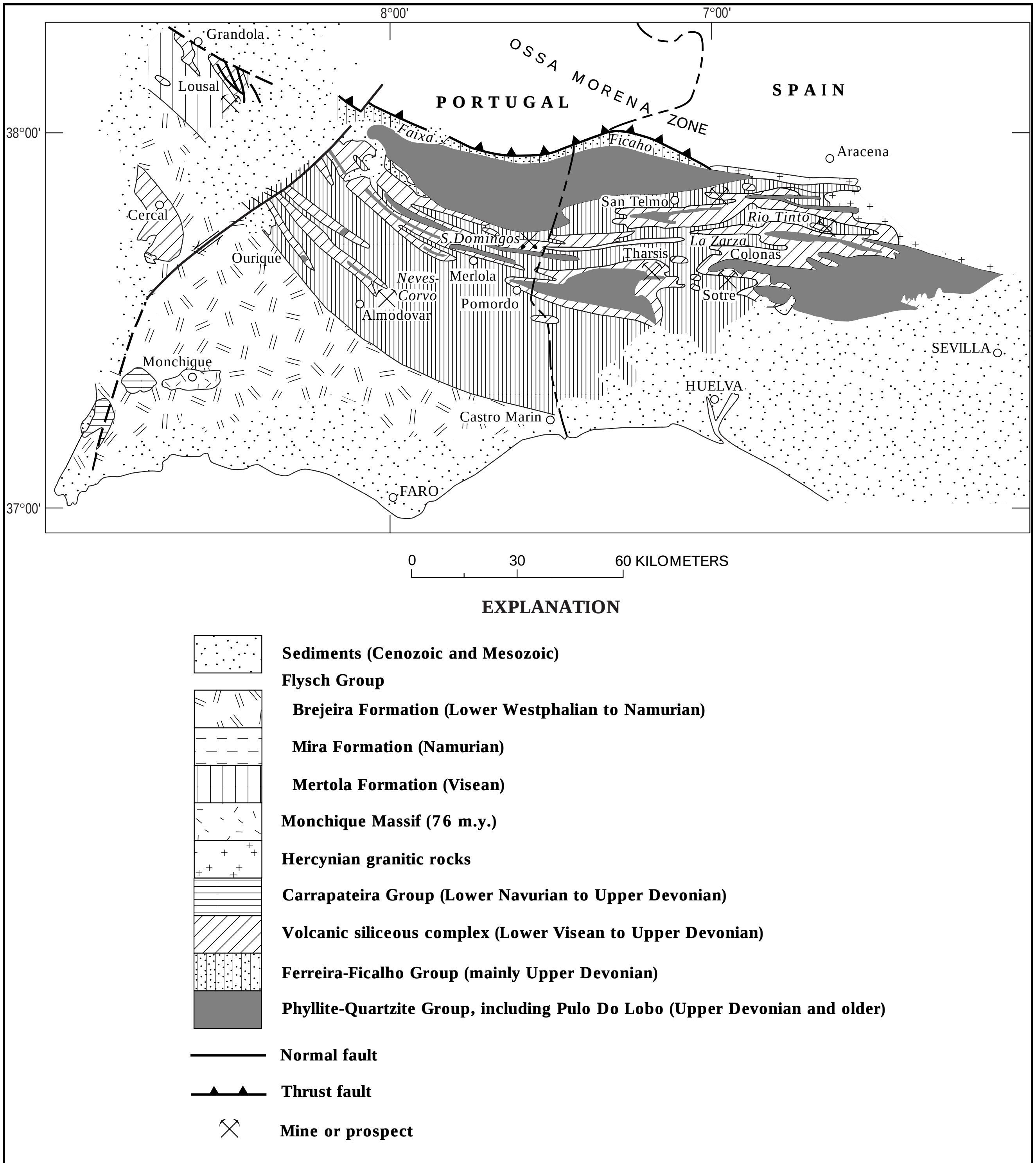

Figure 1. Generalized geologic map of the Iberian Pyrite Belt. Modified from Carvalho (1991).

The IPB forms the main part of the South Portuguese Zone (SPZ), a major tectonostratigraphic province in the Iberian segment of the Hercynian Fold Belt (Lotze, 1945; Ribeiro and others, 1979). Upper Paleozoic rocks of the SPZ correlate with those in the Rhenohercynian Zone of the Hercynian Orogeny in southwestern Ireland and southern England. The SPZ is separated from the Ossa-Morena Zone (OMZ) to the north by an accretionary margin that is characterized in part by dismembered ophiolite terranes. The OMZ is composed of polymetamorphic Precambrian basement and overlying Cambrian to Permian rocks.

The rocks in the PPB are divided into three major lithostratigraphic units which, from oldest to youngest are as follows: (1) Phyllite-Quartzite Group (PQ), (2) Volcanic-

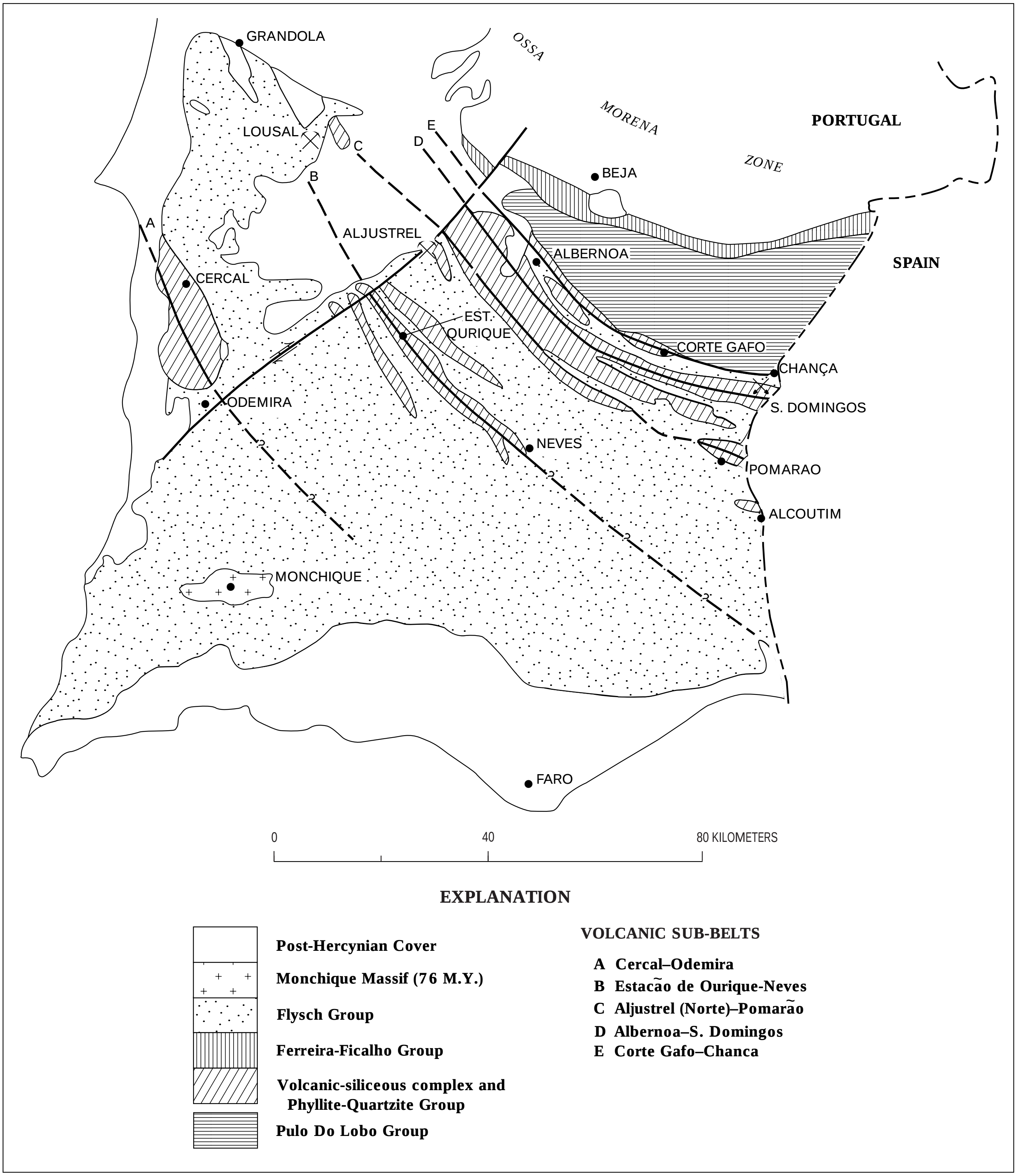

Figure 2. Generalized geologic map of the Portuguese Pyrite Belt showing general trends of 5 volcanic sub-belts. Modified from Carvalho (1991).

siliceous Complex (VS), and (3) Culm or Flysch Group. The oldest unit (PQ) is composed of Devonian shallow marine phyllite and quartzite rocks that crop out along anticlinal axes. This unit is overlain by a mafic to felsic bimodal sequence of volcanic rocks and associated sedimentary rocks (VS) that were deposited primarily in a submarine setting; felsic volcanic rocks are dominant and range in composition from rhyolite to quartz keratophyre. About 20 percent of the volcanic rocks consist of spilitic pillow basalt. Dacite and andesite constitute only a minor part of the volcanic sequence. In addition to the volcanic rocks, the VS unit contains sedimentary rocks primarily at or near the top of the volcanic sequence; these include chemical sedimentary rocks (exhalites) composed of green, red, and gray chert, and bedded barite deposits. The exhalites are commonly intercalated with siliceous tuffaceous beds and vitric tuff. Thin sequences and lenses of epiclastic rocks are interbedded or overlie the exhalites. An Early Visean and Namuro-Westphalian diachronous flysch sequence (Flysch Group) overlies the volcanic rocks; this unit was derived from rocks in the Ossa-Morena Zone and represents the youngest rocks in the PPB. The stratigraphy of this flysch sequence varies from one sub-belt to another and the rock types include shale, graywacke, siltstone, phyllite, and locally conglomerate. A large percentage of the PPB is covered by this thick and monotonous sedimentary sequence.

The dominantly explosive nature of the volcanism that formed many of the rocks in the PPB followed by the development of thick overlying flysch sequences indicate large-scale subsidence. A southwest to northeast migration of the main volcanism has been postulated (Carvalho, 1976; Ribeiro and others, 1979).

The principal tectonic features of the PPB are imbricate thrust faults that displace Paleozoic rocks, and tight to open folds that formed during the Hercynian Orogeny. The earliest deformation resulted from basin subsidence and consisted of synsedimentary faults and slump folds that represent the beginning of the Hercynian Orogeny in the SPZ. Synsedimentary deformation evolved into a compressive tectonic regime of intense folding and thrust faulting resulting in penetrative S1 and, in some cases, S2 cleavages. The intensity of deformation decreased from northeast to southwest; folds in the northeast that are tight to isoclinal are progressively more open to the southwest (Ribeiro and others, 1979; Ribeiro and Silva, 1983). Deformation was accompanied by low-grade regional metamorphism that ranges from zeolite facies in the south to lower greenschist facies in the northeast (Schermerhorn, 1975; Munhá, 1979); much of the PPB is in the prehnite-pumpellyite (lower greenschist) metamorphic facies.

The general lithologic, stratigraphic, and tectonic features of the SPZ suggest that it represents an active convergent margin along which bimodal volcanic rocks were erupted during intermittent extensional regimes in a volcanic arc setting.

Small to very large polymetallic sulfide ore bodies throughout the PPB are hosted by felsic volcanic rocks of largely pyroclastic origin that were deposited during Late Devonian time. Original sulfide ore deposition is estimated at more than 1.5 billion tons (Carvalho, 1991). Of this amount, 20 percent has been mined, and 10 to 15 percent may have been lost as a result of erosion. Current resources and reserves of more than 900 million tons are about equally divided between the Portuguese and Spanish parts of the IPB.

Mining for copper and precious metals in the IPB began more than 3,000 years ago, and copper, zinc, tin, iron, sulfur, and associated gold and silver presently are mined. The largest and highest grade polymetallic deposits are those at Neves-Corvo (Carvalho, 1991). In addition to the polymetallic sulfides, the PPB contains minable manganese and barite.

ACKNOWLEDGMENTS

This project was funded principally by the Luso American Development Foundation which we gratefully acknowledge. Other financial support, as well as technical and logistical assistance, was provided by the U.S. Geological Survey, the Direcção Geral de Geologia e Minas, and its agencies, the Serviços Geológicos de Portugal (SGP), and the Serviço de Fomento Mineiro (SFM).

Delfim de Carvalho, Director of the SGP, was the project coordinator and provided guidance in the field to the USGS scientists assigned to the project. Jose Oliveira of the SGP and Vitor Oliveira of the SFM also provided invaluable support. We wish to thank the many staff members in the offices of the SGP in Lisbon and the SFM in Beja for logistical assistance, hospitality, technical advice, and access to numerous reports. Drafting support was provided by the offices of the SGP in Lisbon. Paulo Castro, SGP, conducted field investigations in the Mombeja area as part of this project.

The cooperation of the companies, Somincor and Pirites Alentejanas greatly contributed to the success of the project. We particularly acknowledge the contributions by David Richards and Pedro Carvalho, of Somincor, and Jose Leitão, of Pirites Alentejanas.

CHAPTER A

RARE EARTH ELEMENT DISTRIBUTION IN THE VOLCANIC LITHOSTRATIGRAPHIC UNITS OF THE PORTUGUESE PYRITE BELT

By David J. Grimes[1], Robert L. Earhart[1], *and* Delfim de Carvalho[2]

INTRODUCTION

Rare earth elements (REE) were determined for samples of volcanic rocks collected in the Portuguese Pyrite Belt during the present studies in order to (1) evaluate REE as a tool for correlating volcanic events, and (2) determine the mobility of REE and assess their use as hydrothermal tracers. The host rocks of the massive sulfide deposits in the PPB are felsic volcanic rocks. Because these rocks are widespread in the PPB, knowledge of the geochemical signatures of the most favorable massive sulfide deposit hosts may directly and indirectly help in the process of selecting or prioritizing exploration targets.

Distribution of mobile REE elements in volcanic rocks can be correlated with the degree of alteration in geologic terranes favorable for massive sulfide deposits (Campbell and others, 1984; Graf, 1977). According to Graf (1977), the coherent and somewhat predictable geochemical properties of REE can be used as tracers to identify alteration reactions in massive sulfide systems. Studies of REE in massive sulfide terranes in eastern Canada have determined a specific reaction sequence (Graf, 1977); these studies provide a better understanding of the genesis of massive sulfide deposits in volcanic rocks of the region. Campbell and others (1984) suggest that the degree of REE mobility may increase with the size of a deposit. If this proves to be true, it would impact the exploration efforts for massive sulfide deposits in the Portuguese Pyrite Belt.

Forty samples were collected from five sub-belts in the PPB and were analyzed for REE (table 1). Each sample was analyzed for elements using an instrumental neutron activation analysis (INAA) method described by Baedecker and McKown (1987) at the U.S. Geological Survey in Denver, Colo. Results of 4 basalt and 19 rhyolite samples were plotted to determine possible REE mobilization trends that might serve as geochemical tracers in the exploration for massive sulfide deposits.

[1]U.S. Geological Survey
[2]Serviços Geológicos de Portugal

A geochemical method to distinguish among volcanic events (lithologic units representative of particular volcanic events) may be a useful exploration tool in the common cases where the more important ore deposits are the products of particular volcanic events. The felsic volcanic rocks in the PPB were originally deposited on the sea floor. The resulting REE pattern is a mixture of REE from magmatic sources and REE from the sea water. In multiple volcanic events, such as those represented in the PPB, the degree of variation from one event to another may be reflected in physical or chemical differences; theoretically, each sequence of rocks may have a unique REE signature.

To test this hypothesis, samples of altered and unaltered volcanic rocks from all of the sub-belts of the PPB were collected and analyzed for REE. Sample descriptions are given in table 1 and the locations of the sub-belts are shown on figure 2.

GEOLOGIC CONSIDERATIONS

According to Carvalho (1972, 1976), the sub-belts of the PPB represent a migration of volcanism associated with collisional processes from south to north during the Hercynian Orogeny, near the end of Paleozoic time. Oliveira (1990), on the other hand, has argued that the volcanic sub-belts developed from north to south. Another interpretation is that some sub-belts may be equivalent in age and the present configuration is the result of structural separation.

In each of the sub-belts, quartz keratophyre is the dominant volcanic rock, and minor amounts of andesite and spilitic basalt are present. Data collected as part of the present study suggest that REE contents show a pattern of depletion from south to north that may be related to the development of the sub-belts. For example, chondrite-normalized data for both light rare earth elements (LREE) and heavy rare earth elements (HREE) in quartz keratophyre show a pattern of depletion from south to north Neves-Corvo to São Domingos (fig. 3*B*); the trend of LREE in

Table 1. Descriptions and locations of samples analyzed for rare earth elements, Portuguese Pyrite Belt.

Sample No.	Area	Volcanic Sub-Belt[1]	Rock Type
P13	Pomarão	C	Felsic volcanic, lower
P9	Pomarão	C	Felsic volcanic, middle
P18	Pomarão	C	Felsic volcanic, upper
P7CE1	Cercal	A	Felsic volcanic, sericitic
P7SL13	Cercal	A	Felsic volcanic, K-altered
P7CE2	Cercal	A	Spilitic basalt
RS8342	Cercal	A	Spilitic basalt
P27	Aljustrel	C	Pillow basalt
P7CV1	Caveiro mine	C	Felsic volcanic
P7LO1A	Lousal	C	Spilitic basalt
P7LO4	Lousal	C	Spilitic basalt, pillowed
P7NC3	Neves-Corvo	B	Felsic volcanic, weakly altered
P7NC4	Neves-Corvo	B	Felsic volcanic, highly altered
P7NC5	Neves-Corvo	B	Felsic volcanic, weakly altered
P7CH1	Chança	E	Felsic volcanic
P7CH10	Chança	E	Felsic volcanic, altered
CA1380	Neves-Corvo	B	Spilitic basalt
P7N9	Castro Verde	B	Spilitic basalt
FS11361	Aljustrel	C	Felsic green tuff, altered
AJ1357	Aljustrel	C	Felsic volcanic, pyritic
P7PA1	Aljustrel	C	Pillow basalt
P7SD13	Sao Domingos	D	Spilitic basalt, chloritic
P7SD14	Sao Domingos	D	Felsic volcanic, vitric, upper
P7SD15	Sao Domingos	D	Felsic volcanic, middle
P7SD18	Sao Domingos	D	Andesite
P7SD21	Sao Domingos	D	Felsic volcanic
P7SD23	Sao Domingos	D	Amygdaloidal basalt
P7SD25	Sao Domingos	D	Felsic volcanic, perlitic
P7CG3	Corte Gafo	E	Felsic volcanic
P7CG6	Corte Gafo	E	Felsic volcanic, weakly altered
P7SB3	Serra Branca	E	Spilitic basalt
P7EO2	Estação Ourique	B	Felsic volcanic
P7CA5	Caseval	B	Amygdaloidal basalt
P7CA7	Casaval	B	Felsic volcanic
P7JM5	Juliana	D	Felsic volcanic
P7JM6	Juliana	D	Andesitic volcanic
P7JM7	Juliana	D	Felsic volcanic
P7AB1	Albernoa	D	Quartz-diorite(?)
P7AB2	Albernoa	D	Felsic volcanic, upper
P7AB3	Albernoa	D	Felsic volcanic, lower

[1]A, Cercal-Odemira; B, Estação de Ourique-Neves; C, Aljustrel-Pomarão; D, Albernoa-Sao Domingos; E, Corte Gafo-Chança

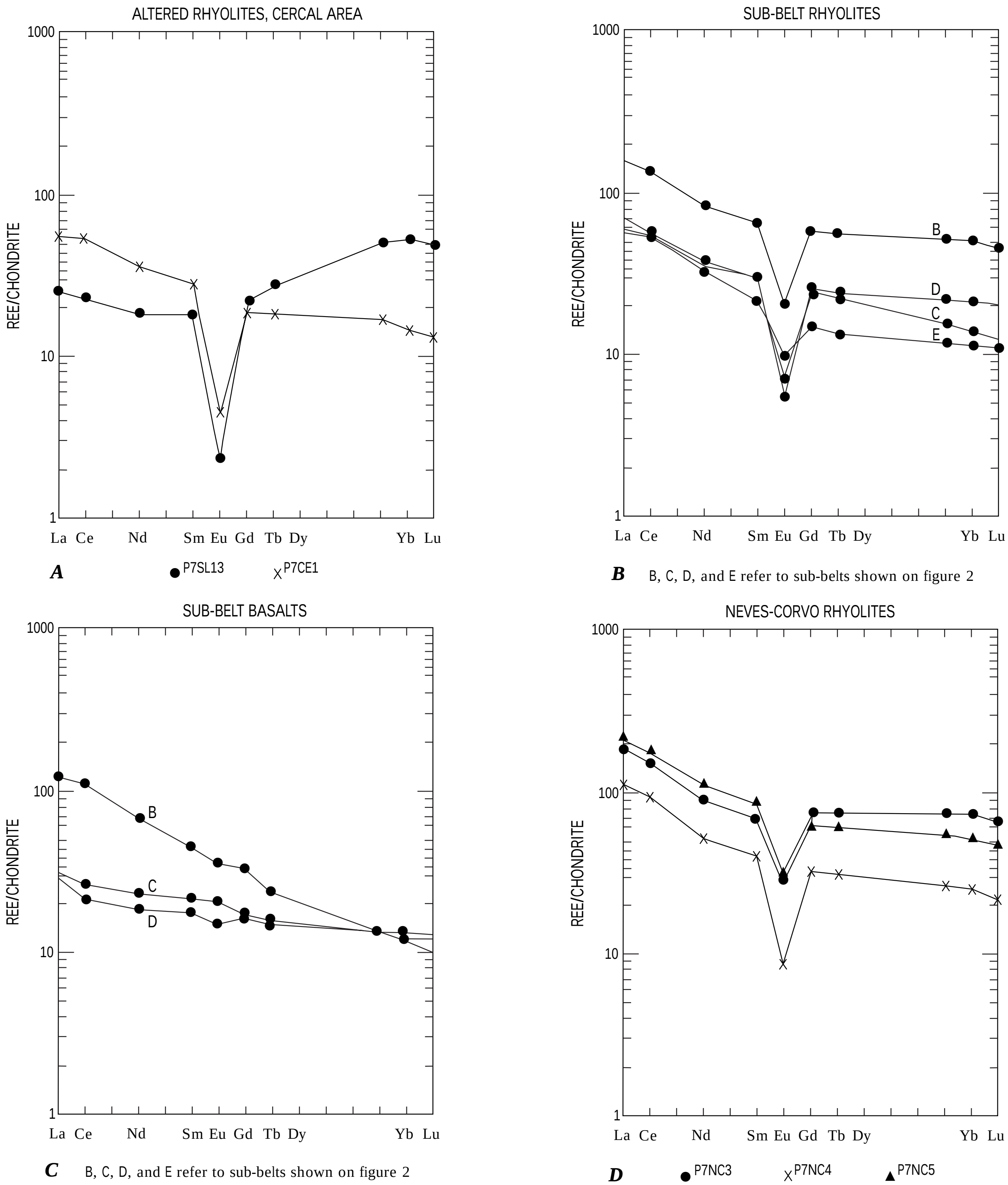

Figure 3 (above and facing page). Chondrite normalized distributions of rare earth elements in volcanic rocks in the Portuguese Pyrite Belt. *A*, altered Cercal rhyolites; *B*, rhyolites from sub-belts B, C, D, and E shown on fig. 2; *C*, basalts from sub-belts B, C, and D shown on fig. 2; *D*, Neves-Corvo rhyolites, and E, basalts and rhyolites.

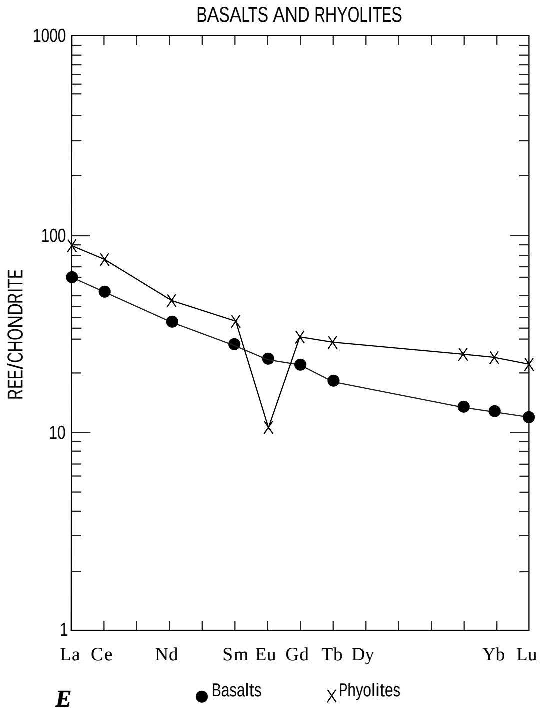

E

spilitic basalt is the same (fig. 3*C*). Quartz keratophyres collected from Juliana near Aljustrel in the north to Casavel near Est. Ourique in the south also show a depletion trend from south to north in both LREE and HREE (figs. 2, 3*B*).

Volcanogenic sulfide occurrences were identified in all five sub-belts; the composition and character of the occurrences, however, varies from deposit to deposit and from sub-belt to sub-belt. The deposits with the highest grade ore occur in the Albernoa-São Domingos sub-belt and the Estaço de Ourique-Neves sub-belt. The deposits with the richest massive sulfide ore are the Neves-Corvo deposits in the southern Estação de Ourique-Neves sub-belt (Carvalho, 1991).

RARE EARTH ELEMENT GEOCHEMISTRY

ALTERED RHYOLITES, CERCAL AREA

For the purpose of this discussion the term “rhyolite” is used to describe siliceous volcanic rocks whose probable average composition approximates that of quartz keratophyre. Two samples of altered rhyolite (nos. P7SL13, P7CE1) from the Cercal area in the western part of the PPB were analyzed for REE and the chondrite-normalized plots are shown in figure 3*A*. Both samples have a high percentage of silica (77.7 percent) quartz keratophyres and are from the upper part of the silicic volcanic sequence near the contact with overlying volcanic-sedimentary rocks of the upper part of the Volcanic-Siliceous Complex. The stratigraphic relationship of the two samples is uncertain; however, they may represent a single volcanic event. Sample no. P7SL13, from the São Luis quarry, is potassically altered, whereas sample P7CE1, from a road cut near the quarry, is intensely sericitically altered. Generally rocks classified as potassically altered are characterized by abundant veinlets of coarse, pink potassium feldspar and those sericitically altered contain abundant sericite throughout the rock. The distribution of REE in the two samples is significantly different; if the two samples represent a single volcanic event, the difference the REE plots suggests that the mobility of REE is related to alteration.

The REE pattern of the sericitically altered sample no. P7CE1 is similar to the average chondrite-normalized REE pattern for PPB rhyolites; the LREE are enriched, europium is depleted, and the La/Yb ratio is 5.93 (table 2, fig. 3*A*). However, the overall REE abundances are lower than the average rhyolite in the PPB and the Eu/Sm ratio is 0.06, lower than the average 0.11. In sample no. P7SL13, LREE are depleted and HREE are relatively enriched as compared to REE in sample no. P7CE1. In contrast, sample no. P7SL13 has a La/Yb ratio of 0.75 and Eu/Sm ratio of 0.05. Similar REE trends in alteration zones associated with a Canadian massive sulfide deposit were identified by Campbell and others (1984); there was an overall depletion of REE, a marked increase in the europium negative anomaly, and the HREE were enriched.

SUB-BELT RHYOLITES

Chondrite-normalized REE determinations of 12 relatively unaltered rhyolite samples from sub-belts B, C, D, and E were plotted using the data shown in table 3 and the distribution patterns indicate high REE abundances (fig. 3*B*). In addition, the LREE are relatively enriched as compared with the HREE, and europium shows a negative anomaly. The enrichment of REE is relatively greater in sub-belt B suggesting that these rhyolites are the “most evolved” of any sub-belt, and the relative depletion of REE in sub-belt E suggests that these rhyolites are the most primitive. Additional evidence suggesting sub-belt B rhyolites are a later stage of magmatic evolvement include the existence of elements

Table 2. Rare earth element concentrations in volcanic rocks, Portuguese Pyrite Belt.

[Leaders (---) indicate no data]

Sample	Cercal rhyolites		Sub-belt basalts					Neves-Corvo rhyolites		
			Sub-belt B	Sub-belt C			Sub-belt D			
No. ----	P7SL13	P7CE1	P7N9	P7LO1A	P7LO4	(Avg.)	P7SD13	P7NC3	P7NC4	P7NC5
Element										
La (ppm)	7.99	17.50	37.70	9.38	10.30	9.84	8.88	57.30	35.00	64.30
Ce (ppm)	18.90	43.70	88.70	19.10	23.60	21.35	17.40	122.00	76.00	141.00
Nd (ppm)	11.10	21.60	40.30	12.50	15.40	13.95	11.30	53.50	31.20	66.90
Sm (ppm)	3.56	5.50	8.77	3.92	4.64	4.28	3.51	13.50	7.99	16.70
Eu (ppm)	.17	.33	2.61	1.42	1.67	1.55	1.10	1.98	.66	2.21
Gd (ppm)	5.63	4.90	8.63	4.17	4.87	4.52	4.30	19.70	8.55	16.10
Tb (ppm)	1.27	.85	1.12	.71	.78	.75	.71	3.51	1.49	2.85
Tm (ppm)	1.59	.54	---	.43	---	.43	.44	2.42	.88	1.78
Yb (ppm)	10.70	2.95	2.51	2.67	2.94	2.81	2.55	15.60	5.38	10.80
Lu (ppm)	1.50	.41	.33	.38	.45	.42	.40	2.13	.71	1.55
SiO_2 (%)	77.70	77.70	45.0	45.2	45.2	45.2	48.7	74.00	75.10	71.70
Element Ratios										
La/Yb	.75	5.93	15.02	3.51	3.50	3.51	3.48	3.67	6.51	5.95
Eu/Sm	.05	.06	.30	.36	.36	.36	.31	.15	.08	.13

Table 3. Rare earth element concentrations in sub-belt rhyolites, Portuguese Pyrite Belt.

	Sub-belt B					Sub-belt C				Sub-belt D			Sub-belt E			
Sample No.	P7NC3	P7NC4	P7NC5	P7EO2	(Avg.)	P9	P13	P7CV1	(Avg.)	P7SD14	P7SD15	(Avg.)	P7CH1	P7AB2	P7AB3	(Avg.)
Element																
La (ppm)	57.30	35.00	64.30	43.80	50.10	27.60	13.10	16.80	19.17	17.80	18.20	18.00	19.20	21.50	26.00	22.23
Ce (ppm)	122.00	76.00	141.00	104.00	110.75	63.30	33.30	39.50	45.37	41.70	46.40	44.05	40.30	47.80	51.80	46.63
Nd (ppm)	53.50	31.20	66.90	50.30	50.48	28.30	17.90	17.80	21.33	24.00	21.20	22.60	17.60	22.00	20.00	19.87
Sm (ppm)	13.50	7.99	16.70	13.30	12.87	6.80	5.79	5.33	5.97	6.12	5.40	5.76	4.00	4.72	4.14	4.29
Eu (ppm)	1.98	0.66	2.21	1.24	1.52	0.56	0.65	0.39	0.53	0.43	0.39	0.41	0.82	0.68	0.69	0.73
Gd (ppm)	19.70	8.55	16.10	15.90	15.06	6.66	7.53	5.00	6.40	6.80	6.59	6.70	4.10	3.90	3.66	3.89
Tb (ppm)	3.51	1.49	2.85	2.59	2.61	1.00	1.31	0.85	1.05	1.10	1.16	1.13	0.64	0.64	0.60	0.63
Tm (ppm)	2.42	0.88	1.78	1.56	1.66	0.62	0.49	0.38	0.50	0.57	0.83	0.70	0.36	0.39	0.39	0.38
Yb (ppm)	15.60	5.38	10.80	9.51	10.32	3.78	2.51	2.32	2.87	3.50	5.24	4.37	2.20	2.40	2.40	2.33
Lu (ppm)	2.13	0.71	1.55	1.30	1.42	0.55	0.32	0.30	0.39	0.49	0.80	0.65	0.33	0.36	0.35	0.35
SiO2 (%)	74.00	75.10	71.70	77.40	74.55	82.00	77.10	74.60	77.90	80.9	79.20	80.05	71.70	76.4	77.30	75.13
Element Ratios																
La/Yb	3.67	6.51	5.95	4.61	4.85	7.30	5.22	7.24	6.68	5.09	3.47	4.12	8.73	8.96	10.83	9.53
Eu/Sm	0.15	0.08	0.13	0.09	0.12	0.08	0.11	0.07	0.09	0.07	0.07	0.07	0.21	0.14	0.17	0.17

Table 4. Hafnium, tantalum, and zirconium concentrations in sub-belt rhyolites, Portuguese Pyrite Belt.
[Average concentrations in ppm]

Element	Sub-belts			
	B	C	D	E
Hf	9.3	3.8	3.8	5.6
Ta	1.5	.96	1.0	.82
Zr	360	121	108	210

which do not readily substitute into the crystalline lattice of major rock forming minerals, such as hafnium, tantalum, and zirconium, occurring in relatively higher amounts in sub-belt B rhyolites (table 4).

Rhyolites from sub-belts C and D have more pronounced negative europium anomalies than sub-belts B and E. Eu/Sm ratios in the sub-belts are as follows C, 0.07; D, 0.09; B, 0.12; and E, 0.17. Sub-belts C and D rhyolites have higher SiO_2 concentrations than sub-belt B and E rhyolites. Two theories on what the increase in the relative abundances of the HREE and the decrease in the La/Yb ratio in samples from sub-belts E to B (table 3) may mean include the following: (1) local fractional crystallization or a higher magmatic evolvement from sub-belt E to sub-belt B, as proposed by Munhá, (1983), or (2) the differences in relative abundances of the REE may be related to post-magmatic alteration effects.

NEVES-CORVO RHYOLITES

Samples of three rhyolite units that represent separate felsic volcanic events were collected from the underground workings in the Neves-Corvo mine. Chondrite-normalized plots of the REE concentrations of the three samples (nos. P7NC3, P7NC4, P7NC5), are shown on figure 3*D*. Sample no. P7NC4 is from the stratigraphic top of the volcanic pile; it is closely associated with the massive sulfide deposit and of the three samples is the most intensely sericitically altered indicating a weak sericitic alteration effect. We believe that the REE distributions reflect the degree of alteration (table 2). Samples nos. P7NC3 and P7NC5 have Eu/Sm ratios of 0.15 and 0.13, respectively. The HREE are relatively enriched in sample no. P7NC3 as compared to the HREE in sample no. P7NC5; the La/Yb ratio for sample no. P7NC3 is 3.67 and for sample no. P7NC5 in 5.95. Concentrations of other incompatible elements for sample nos. P7NC5 and P7NC3 are as follows: Hf, 13.6 ppm and 13.7 ppm; Ta, 1.9 ppm and 1.9 ppm; and Zr, 523 ppm and 525 ppm and suggest the samples experienced similar degrees of magmatic evolvement. The REE distribution pattern of sample no. P7NC4, the more highly altered sample, contrasts sharply with REE distribution patterns of the other two samples on the chondrite-normalized plot (fig. 3*D*); the REE abundances are lower, the europium negative anomaly is greater, and the Eu/Sm ratio is 0.08. In addition, concentrations of other incompatible elements in sample no. P7NC4 are much lower than those in the other two less altered samples; Hf, 3.4 ppm, Ta, 0.84 ppm, and Zr, 150 ppm. These differences may indicate that the rhyolite in sample no. P7NC4 is less evolved than the other samples or that REE were depleted through hydrothermal alteration.

SUB-BELT BASALTS

Chondrite-normalized diagrams showing the REE distributions in basalts from sub-belts B, C, and D (fig. 3*C*) are based on the analytical data shown in table 2. The results from sub-belts C and D samples, are similar in that only slight enrichment of the LREE with respect to the HREE occurs (fig. 3*C*) and La/Yb ratios are about 3.5. REE distribution patterns of samples from sub-belts C and D are similar to samples of continental tholeiite (Cullers and Graf, 1984), and to lower mafic lava samples from the PPB described by Munhá (1983). The chondrite-normalized plot for basalt samples from sub-belt B is distinctly different from the plots for basalt samples from sub-belts C and D. The results plotted for sub-belt B samples show a steeper slope, are relatively enriched in LREE, and have a La/Yb ratio of more than 15, a pattern that closely resembles the REE plots of alkali basalts reported by Cullers and Graf (1984) and the upper mafic lavas (type-B dolerites) reported by Munhá (1983). These results from basalt samples suggest that REE patterns from sub-belts C and D are more primitive and the basalt samples from sub-belt B are more evolved. The relative enrichment of the LREE in sub-belt B basalt samples may be related to fractional crystallization or may have resulted from contamination by the assimilation of rocks in the upper crust and detailed petrographic studies are needed to interpret the results.

RARE EARTH ELEMENT AVERAGES, BASALTS AND RHYOLITES

The average normalized-chondrite distribution patterns of 4 basalt and 12 rhyolite samples collected from the PPB are similar (fig. 3*E*). The rhyolites contain higher REE abundances and show more distinct negative europium anomalies than the basalts. The slope and distribution patterns are comparable to those of alkali basalts and related felsic rocks studied by Cullers and Graf (1984); the REE pattern of the basalt samples is also similar to patterns for lower mafic lava in the PPB (Munhá, 1983). The REE pattern for PPB rhyolite samples falls between those for the rhyolite samples analyzed by Munhá (1983) and high-silica rhyolite samples. Although the basalt and rhyolite plots suggest that the PPB rhyolites may be derived from fractional crystallization of basaltic magma, additional samples of relatively unaltered rhyolite rocks from throughout the PPB need to be analyzed before such a conclusion could be confirmed.

CONCLUSIONS AND RECOMMENDATIONS

Rare earth element distributions in sub-belt rhyolite and basalt samples show relative enrichment from north to south in the PPB which may be the result of fractional crystallization of the parent magma or the result of contamination by partial melting of upper crustal rocks. If the REE enrichment is related to fractional crystallization, and the development of sub-belt volcanic rocks can be proven to have progressed from north to south, the usefulness of REE distributions as a tool for correlating and distinguishing volcanic events will be demonstrated. However, additional REE data are needed to confirm this hypothesis of development in the PPB.

Variations in the distribution of REE in altered felsic volcanic rocks in the Cercal and Neves-Corvo areas seem to reflect the degree of rock alteration. A sample of potassically altered rhyolite from a quarry near Cercal contained REE abundances that were significantly different from less-altered rhyolite samples collected nearby. In addition, the REE chondrite-normalized plot of an intense sericitically altered rhyolite sample collected from the top of the volcanic pile and closely associated with the massive sulfide deposits at Neves-Corvo, had depleted REE abundances as compared to plots of similar samples collected from a lower part of the volcanic pile from different localities. If these differences prove to be related to an increase in the mobility of REE as a result of hydrothermal alteration, REE will be shown as useful hydrothermal tracers or as geochemical indicators of favorable host rocks for massive sulfide deposits. Additional work is needed to confirm these findings.

CHAPTER B

GEOLOGIC SETTING AND GEOCHEMICAL CONTROLS ON THE DISTRIBUTION OF GOLD IN THE PORTUGUESE PYRITE BELT

By Robert L. Earhart[1], Delfim de Carvalho[2], Vitor Oliveira[3], Jose T. Oliveira[2], *and* Paulo Castro[2]

INTRODUCTION

The geologic setting and distribution of gold and associated elements in the Portuguese Pyrite Belt (PPB) were studied in order to (1) identify terranes in the PPB that may be favorable for gold occurrences, and (2) develop a geochemical deposit type that will be useful in future gold exploration programs not only in the PPB but in similar geologic terranes worldwide. Exploration for gold deposits in the PPB was not an objective in these studies.

The development of a deposit model for gold in the PPB involved geologic reconnaissance mapping using existing geologic maps and reports. Additional geologic data were collected during the summers of 1987 and 1988; core from drill holes were examined and sampled in areas that had been explored for massive sulfide deposits. Rock outcrop and drill core samples were collected from areas identified as permissive for gold and associated elements. Lists of analytical data are included in Appendix A. Samples were analyzed using an atomic absorption-graphite furnace method in which the lower limit of detection for gold is 2 parts per billion (ppb) (Meier, 1980). Other elements commonly associated with gold were analyzed using an inductively coupled plasma emission spectrographic method (Motooka and Sutley, 1982). Correlation coefficients of selected elements were obtained using the computer program Minitab (table 5). For statistical compilations, analytical results of samples with qualified values, that is, not detected at the lower limit of determination (N), and detected, but below limit of determination (L), are assigned a value at the lower limit of detection.

In many parts of the world, geologic environments similar to those in and near the PPB contain gold in massive sulfide deposits and spatially associated volcanic, chemical sedimentary (exhalites), and in ultramafic rocks that range from Archean to Tertiary in age. Mining areas where gold deposits are spatially or genetically associated with rocks in massive sulfide terranes include the Timmins district, Canada, the Kuroko deposits, Japan (Sato, 1966), and the Tasmanian deposits in Australia (Huston and Large, 1989).

Gold deposits that occur in ultramafic rocks are not necessarily genetically associated with massive sulfide deposition, but are frequently associated with the tectonic belts along continental margins that contain massive sulfides in rocks of magmatic arc derivation. Some well known examples of ultramafic rocks forming in extensional structures along the accreted margin of colliding oceanic and continental plates include the Larder Lake Break in eastern Canada and the Melones Fault, California.

In tectonic belts along accreted margins resulting from the collision of oceanic and continental plates, such as the margin between the South Portuguese Zone and the Ossa-Morena, a tripartite spatial association of gold deposits, massive sulfides, and ultramafic rocks may be present. A well documented example is where the gold deposits and ultramafic rocks of the California mother lode are generally adjacent (landward) to the California zinc-copper massive sulfide belt in the foothills of the Sierra Nevada.

Exhalite deposits which are related to the waning stages of volcanism are deposited in island arc (and possibly fore arc) settings. Rocks of exhalative origin are important hosts of gold deposits. Some examples of very large exhalite-hosted gold deposits include algoma-type iron formations, including the Homestake deposit, South Dakota; baritic and siliceous exhalites, including the Hemlo deposit, Canada; and baritic and siliceous exhalites of Tasmania, Australia.

The occurrence of gold and silver in the massive sulfide ores of the IPB is well documented (Strauss and Beck, 1990). Precious metals were recovered by ancient miners from oxidized parts of massive sulfide bodies, and are common byproducts of both oxidized and unoxidized ores in modern mining operations. The current studies are not directed primarily towards the collection of additional geologic and geochemical data related to the distribution of gold in the massive sulfide bodies, but are designed to investigate other subenvironments closely related spatially and, in most cases, genetically to the massive sulfide deposits. The following

[1]U.S. Geological Survey
[2]Serviços Geológicos de Portugal
[3]Serviços de Formento Mineiro

Table 5. —Correlation coefficients, rock samples in Portuguese Pyrite Belt.

Proximal exhalites

	Au	Ag	As	Cu	Pb	Zn	Ba
Au	-	-	-	-	-	-	-
Ag		-	0.322	0.307	0.623	0.602	-0.084
As			-	0.357	0.389	0.585	0.618
Cu				-	0.201	0.254	0.120
Pb					-	0.630	0.145
Zn						-	-0.040
Ba							-

Distal exhalites

	Au	Ag	As	Cu	Pb	Zn	Sb	Mn	Ba
Au	-			0.364	-0.186	-0.032	-0.111	-0.190	-0.186
Ag		-		0.010	-0.256	-0.292	-	0.662	-
As			-	0.187	-0.081	0.514	-0.100	0.459	-0.193
Cu				-	-0.183	0.196	0.783	-0.078	0.010
Pb					-	0.512	-0.090	-0.125	-0.256
Zn						-	-0.045	0.313	-0.292
Sb							-	-0.142	0.290
Mn								-	0.662
Ba									-

All rocks, Chança area

	Au	Ag	As	Cu	Pb	Zn	Bi	Sb	Mo
Au	-	-0.057	0.791	0.568	0.387	-0.188	-0.044	0.515	0.301
Ag		-	0.126	0.005	0.645	0.609	0.382	0.665	-0.026
As			-	0.459	0.484	-0.039	-0.020	0.418	0.168
Cu				-	0.199	-0.037	0.467	0.249	0.116
Pb					-	0.472	0.213	0.693	0.069
Zn						-	0.166	0.359	-0.035
Bi							-	0.213	-0.099
Sb								-	0.315
Mo									-

Felsic volcanic rocks, Salgadinho area

	Au	Ag	As	Cu	Pb	Zn	Bi	Sb	Mo
Au	-	0.780	0.095	0.713	-0.027	-0.097	-0.161	-0.055	-0.061
Ag		-	0.107	0.868	0.024	0.208	-0.219	-0.055	-0.037
As			-	0.211	-0.004	0.458	-0.269	-0.039	-0.080
Cu				-	-0.036	0.242	-0.279	-0.068	-0.084
Pb					-	0.140	0.435	-0.038	0.923
Zn						-	-0.135	-0.059	0.101
Bi							-	0.300	0.563
Sb								-	0.067
Mo									-

Veins and breccias, Salgadinho area

	Au	Ag	As	Cu	Pb	Zn	Bi	Sb
Au	-	-0.028	0.036	0.041	-0.043	0.028	-0.036	-0.092
Ag		-	-0.010	0.956	0.293	0.044	0.983	0.932
As			-	-0.00	-0.159	0.009	-0.039	0.004
Cu				-	0.305	0.094	0.936	0.884
Pb					-	0.826	0.232	0.148
Zn						-	-0.048	-0.137
Bi							-	0.925
Sb								-

Sedimentary rocks, Salgadinho area

	Au	Ag	As	Cu	Pb	Zn	Bi
Au	-	0.436	0.092	0.169	0.318	0.197	0.446
Ag		-	0.020	0.393	0.386	0.159	0.896
As			-	0.052	0.064	0.537	-0.003
Cu				-	0.214	0.079	0.564
Pb					-	0.755	0.587
Zn						-	0.267
Bi							-

Table 5. —Correlation coefficients, rock samples in Portuguese Pyrite Belt—Continued.

Felsic volcanic rocks, Mina de São Domingos

	Au	Ag	As	Cu	Pb	Zn	Bi	Sb	Mo
Au	-	0.039	0.409	-0.002	0.039	-0.114	0.153	-0.063	0.974
Ag		-	0.306	0.574	0.989	-0.145	0.568	-0.053	-0.053
As			-	0.799	0.348	-0.285	0.065	-0.020	0.407
Cu				-	-0.608	-0.172	0.253	0.011	-0.042
Pb					-	-0.168	0.562	-0.054	-0.050
Zn						-	-0.075	-0.188	0.101
Bi							-	-0.068	-0.068
Sb								-	-0.048
Mo									-

Exhalites, Mina de São Domingos

	Au	Ag	As	Cu	Pb	Zn	Bi	Sb	Mo	Mn	Ba
Au	-	0.992	0.556	-0.082	0.794	-0.133	0.998	0.997	0.854	-0.152	0.435
Ag		-		-0.074	0.710	-0.120	0.998	0.979	0.780	-0.133	0.386
As			-	0.402	0.709	0.243	0.528	0.588	0.694	-0.250	0.410
Cu				-	-0.070	0.689	-0.078	-0.087	-0.104	-0.147	0.481
Pb					-	-0.140	0.754	0.840	0.994	-0.213	0.582
Zn						-	-0.127	-0.139	-0.161	0.415	0.235
Bi							-	0.990	0.819	-0.143	0.411
Sb								-	0.892	-0.163	0.462
Mo									-	-0.202	0.559
Mn										-	-0.178
Ba											-

Epiclastic rocks, Mina de São Domingos

	Au	Ag	As	Cu	Pb	Zn	Bi	Mo	Ba
Au	-	-0.078	-0.056	-0.093	0.102	0.132	-0.093	-0.052	0.075
Ag		-	-0.056	0.515	0.063	-0.147	0.882	0.059	-0.063
As			-	0.452	0.119	-0.050	-0.071	-0.060	0.053
Cu				-	-0.114	0.158	0.508	-0.020	-0.235
Pb					-	-0.108	-0.076	-0.024	0.901
Zn						-	-0.165	-0.150	-0.141
Bi							-	-0.071	-0.103
Mo								-	-0.098
Ba									-

Mafic volcanic rocks, Mina de São Domingos

	Au	Ag	As	Cu	Pb	Zn	Sb
Au	-	-	0.324	-0.066	0.016	-0.160	0.377
Ag		-	-	-	-	-	-
As			-	-0.033	0.206	-0.178	0.945
Cu				-	-0.061	-0.109	-0.038
Pb					-	0.009	0.221
Zn						-	-0.130
Sb							-

All rocks, Serra Branca

	Au	Ag	As	Cu	Pb	Zn	Mo
Au	-	0.033	0.205	0.173	0.065	-0.099	-0.058
Ag		-	-0.075	-0.073	-0.088	-0.199	-0.058
As			-	-0.032	-0.045	0.079	0.062
Cu				-	0.872	0.222	0.001
Pb					-	0.402	-0.089
Zn						-	-0.249
Mo							-

Serpentinites, Mombeja

	Cr	Ni	Co	Cu	Zn
Cr	-	0.211	0.202	0.417	-0.007
Ni		-	0.866	-0.173	0.087
Co			-	-0.010	0.696
Cu				-	0.087
Zn					-

Listwaenites, Mombeja

	Cr	Ni	Co	Cu	Zn
Cr	-	0.503	0.386	-0.159	-0.001
Ni		-	0.888	-0.059	-0.312
Co			-	0.145	-0.153
Cu				-	0.013
Zn					-

summary of recent research on the occurrence of gold in massive sulfide deposits presents the possible genetic and spatial interrelationships of gold ores in volcanogenic settings.

GOLD IN MASSIVE AND DISSEMINATED SULFIDE DEPOSITS

GOLD IN MASSIVE SULFIDE DEPOSITS

Gold is commonly recovered as a byproduct in massive sulfide mining operations throughout the world. Gold is the principal ore mined from massive sulfide deposits in some localities; one example is the Mt. Morgan deposit, a late Paleozoic massive sulfide deposit in Queensland, Australia. Mt. Morgan, the largest known gold deposit in Australia, contained 67 million tons of massive sulfide ore, averaging 4.87 g/t gold and 0.7 percent copper (Frets and Balde, 1975) is now mined out. The Horne and Quemont deposits in the Noranda district of Quebec, Canada, also contain large reserves of gold averaging 4.5 g/t (Franklin and others, 1981).

Two distinct types of gold occurrences were recognized by Huston and Large (1989) in massive sulfide deposits in Australia and eastern Canada: (1) gold-zinc-lead-silver association in the zinc-rich upper parts of massive sulfide deposits, and (2) gold-copper association in the lower parts of massive sulfide bodies and in the upper part of the underlying stringer ore. In any single deposit, the gold commonly occurs in one of the settings to the exclusion of the other. In the upper zinc-rich zone, gold is transported in bi-sulfide complexes and gold precipitation is promoted by near neutral, oxidized and low temperature fluids (150°C-275°C); barite-carbonate gangue is present. In the lower zone, gold is transported as chloride complexes at temperatures ranging from 275°C to 350°C. Both the type of gold occurrence and the grade of the ore are controlled by temperature, pH, and the oxygen fugacity of the ore-forming fluids. Empirical data suggest that if gold is present in anomalous concentrations in the copper-rich lower part of a deposit, it will likely be deficient in both the barite-bearing, zinc-rich upper part of the deposit and in the massive to richly disseminated exhalative barite deposits that commonly overlie the massive sulfide deposit. Conversely, if anomalous concentrations of gold are present in the overlying barite-bearing rocks, the lower copper-rich rocks are relatively deficient in gold.

A simplistic diagrammatic model showing gold associations in massive sulfide deposits and adjacent subenvironments of the PPB is shown in figure 4. In and adjacent to the SPZ, the following types of deposits are representative of the subenvironments that may be favorable for the discovery of gold: (1) massive sulfide deposits, (2) disseminated sulfide deposits (referred to locally as “safrão” deposits), (3) chemical sedimentary rocks (exhalites), (4) silicic- and sericitic-altered felsic volcanic rocks, and (5) altered ultramafic rocks (fig. 4). Analytical results of rock samples in or closely related to the massive and disseminated sulfide deposits in the PPB that were investigated during the present studies indicate that gold is more closely associated with the copper-rich rather than with the zinc-rich ores (table 5). Gold in the barite-rich rocks of the IPB is rarely, if ever, present above the lower limit of detection (2 ppb). In contrast, gold ore in the Rosebery deposit, Tasmania, Australia, occurs in both the zinc-rich upper part of the massive sulfide body and in the overlying exhalative massive barite (Huston and Large, 1989); an area near the Black Sea in Turkey is currently being studied by the Geological Survey of Turkey and the gold distribution is similar to that in Tasmania. The occurrence and distribution of gold in exhalite-facies rocks are discussed in greater detail in a following section of this chapter.

GOLD IN DISSEMINATED SULFIDE DEPOSITS

The following two types of disseminated sulfide deposits were investigated in the Portuguese Pyrite Belt: (1) disseminated sulfide deposits in a proximal volcanic setting, such as the sulfide occurrence at Chança on the border between Portugal and Spain (figs. 2, 5), and (2) disseminated sulfides in a distal volcanic setting, such as the sulfide occurrence at Salgadinho in the western part of the PPB (figs. 2, 6). The two settings have distinctly different volcanic and sedimentary stratigraphy, as well as, different positions relative to known volcanic centers.

CHANÇA AREA

The disseminated sulfide occurrence at Chança is characterized by a relatively thick sequence of felsic pyroclastic rocks including abundant coarse fragments that represent proximal deposits of highly explosive volcanism (fig. 5). The felsic volcanic sequence includes pyritic rhyolitic or quartz keratophyric breccia. Epiclastic rocks are rare in the volcanic sequence, but locally tuffite and black shale overlie the volcanic rocks in the upper part of the Volcanic-Siliceous (VS) Complex. These rocks are, in turn, overlain by graywacke and shale that comprise the Flysch Group (fig. 5). Volcanic rocks of the VS Complex are locally present in folded and faulted rocks in the upper plate of a northwest-trending thrust fault. The area also contains subvolcanic rhyolitic intrusive rocks and diabase dikes. Felsic volcanic rocks near the leading edge of the thrust commonly contain richly disseminated sulfide minerals and form a large gossan both in Portugal and Spain in the vicinity of the Chança River. The disseminated sulfides, which consist mostly of

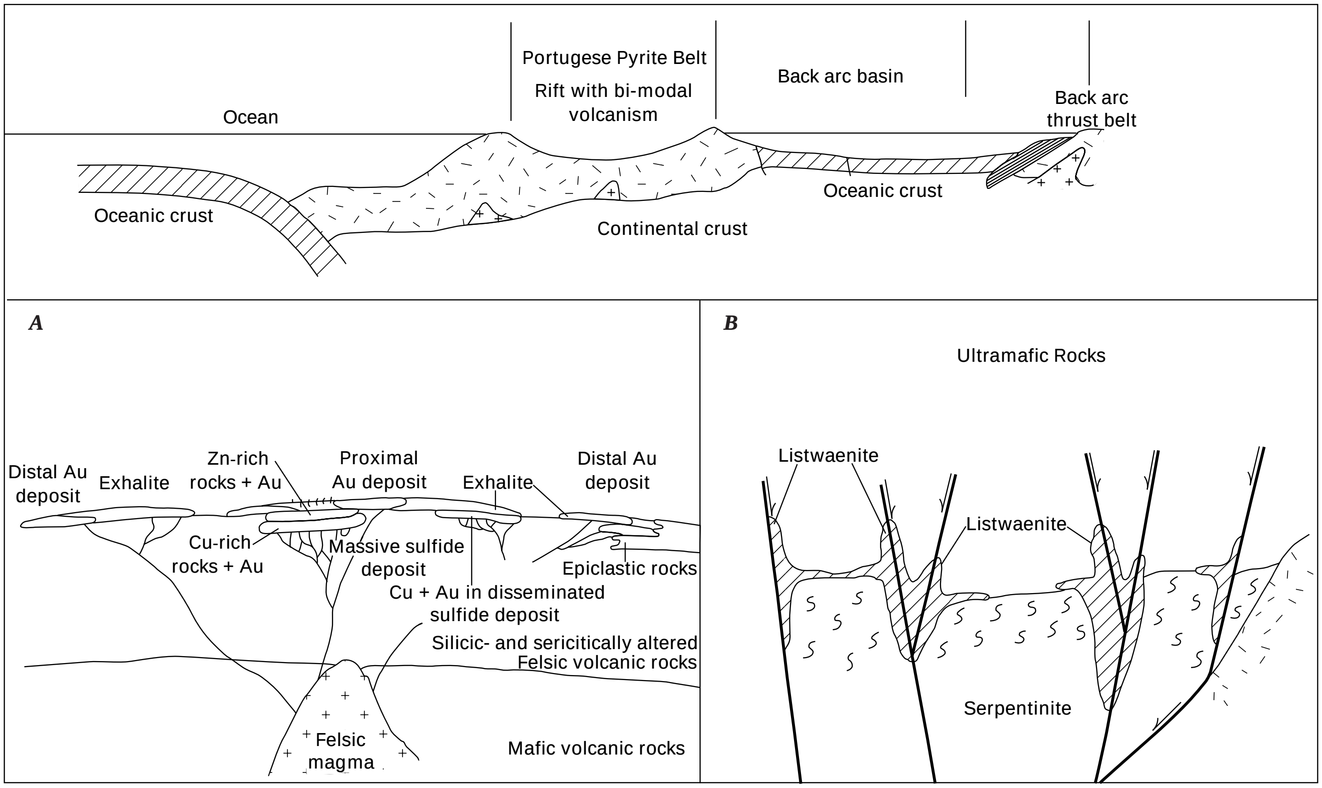

Figure 4. Schematic cross section across the South Portuguese Zone showing tectonic setting and theoretical gold occurrences. Enlarged sections of schematic cross sections of *A*, Portuguese Pyrite Belt and *B*, Mobile Belt. Back arc rocks in South Portuguese Zone preserved only in back arc thrust (Mobile Belt).

pyrite with minor amounts of chalcopyrite, sphalerite, and galena, occur in highly siliceous felsic volcanic rocks in which quartz phenocrysts are commonly preserved. Commonly, the disseminated zone consists of less than 10 percent sulfide minerals; rarely it is known to be as much as 70 percent of the rocks over narrow intervals. The effects of sericitic and chloritic alteration are common in the disseminated sulfide zones. Locally, quartz-sulfide stringer zones are preserved in the more highly chloritic and agglomeratic footwall rocks.

During 1987 and 1988, a total of 62 samples, 31 drill core and 31 outcrop, were collected from the Chança area. The sample localities are shown on figure 5. The samples were primarily silicified, sericitized, and chloritized felsic volcanic rocks.

Anomalous concentrations of gold, as high as 200 ppb, were found in samples of pyrite-rich (as much as 70 percent) and highly siliceous felsic tuff that contained minor amounts of chalcopyrite. Samples with the highest concentrations of gold were collected from the stratigraphically lower part of the stratabound disseminated sulfides and from the upper part of the underlying stringer zone in the footwall. Samples from the Chança area are similar to samples collected from similar deposit types worldwide in that the gold is associated with arsenic, antimony, and copper and there is very little or no zinc (table 5).

Early precipitation of copper during fluid mixing in the plume above the sea floor at high temperatures was explained by Sato (1973) who developed a thermodynamic model based on metal chloride solubilities. In this model, zinc and lead precipitate at lower temperatures. The presence of anomalously high gold in the copper-rich lower parts of the disseminated sulfide body and in the footwall stringer zone at Chança suggests that the gold was precipitated from a chloride complex at temperatures between 275°C and 350°C (Huston and Large, 1989). The geochemical data from the Chança area samples suggest that gold precipitation temperatures were toward the low end of this range. Precipitation of gold in the Chança area was probably triggered by a combination of increasing pH, decreasing oxygen fugacity, and decreasing temperature during the formation of the disseminated sulfides. Geochemical indicators of zones most favorable for gold deposits include Ag, As, Bi, Cu, Mo, Pb, and Sb (table 5) and our studies suggest that the most prospective parts of disseminated sulfide occurrences are copper-rich lower parts.

SALGADINHO AREA

The disseminated sulfide occurrence at Salgadinho (fig. 6) in the western part of the PPB and in the southernmost volcanic sub-belt was deposited in a distal volcanic setting. This

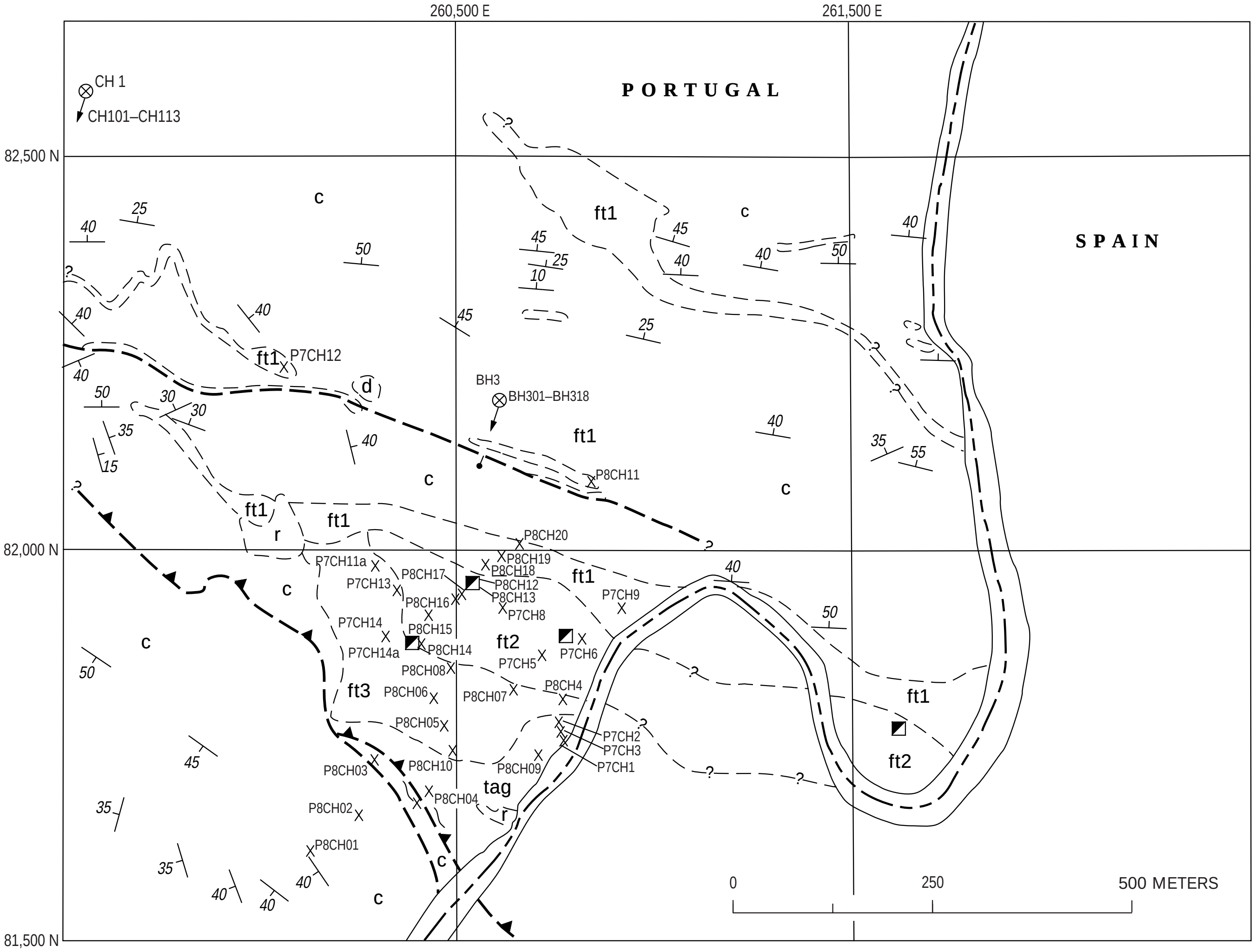

EXPLANATION

Intrusive rocks

d	**Diabase dike**
r	**Rhyolite-rhyodacite**

Extrusive and sedimentary rocks

Culm Group

c	**Turbidites consisting of shale, siltstone, and quartzite, intercalated felsic pyroclastic rocks**

Volcanic-siliceous complex

ft1	**Felsic tuff, unit 1**—Intense to moderate sericitic alteration, weak to moderate iron hydroxide and iron sulfate minerals, interbedded tuffite, shale, and minor chert
ft2	**Felsic tuff, unit 2**—Locally agglomeratic, abundant iron hydroxide and iron sulfate minerals, commonly silicified, forms gossan
ft3	**Felsic tuff unit 3**—Locally agglomeratic, commonly chloritic, quartz veinlets locally, highly deformed. Limonite and copper carbonate minerals in fractures
tag	**Felsic agglomerate and tuff**—Highly chloritic, highly deformed, quartz and calcite veinlets with oxidized sulfide minerals, by purple shale of the Borra do Vinho Formation

Contact—Inferred. Queried where uncertain

Strike and dip of beds (50)

Shear zone

Normal fault—Inferred, bar and ball on downthrown block

Thrust fault—Inferred, bar and ball on downthrown block. Queried where uncertain

Drill hole—Showing number, direction, and sample numbers (CH 1, CH101–CH113)

Rock sample locality—Showing number (P7CH1)

Shaft

Adit

International boundary

Figure 5. Geologic map of the Chança area showing drill hole and rock sample localities. Modified from Billiton Portuguesa and Serviços Geológicos de Portugal.

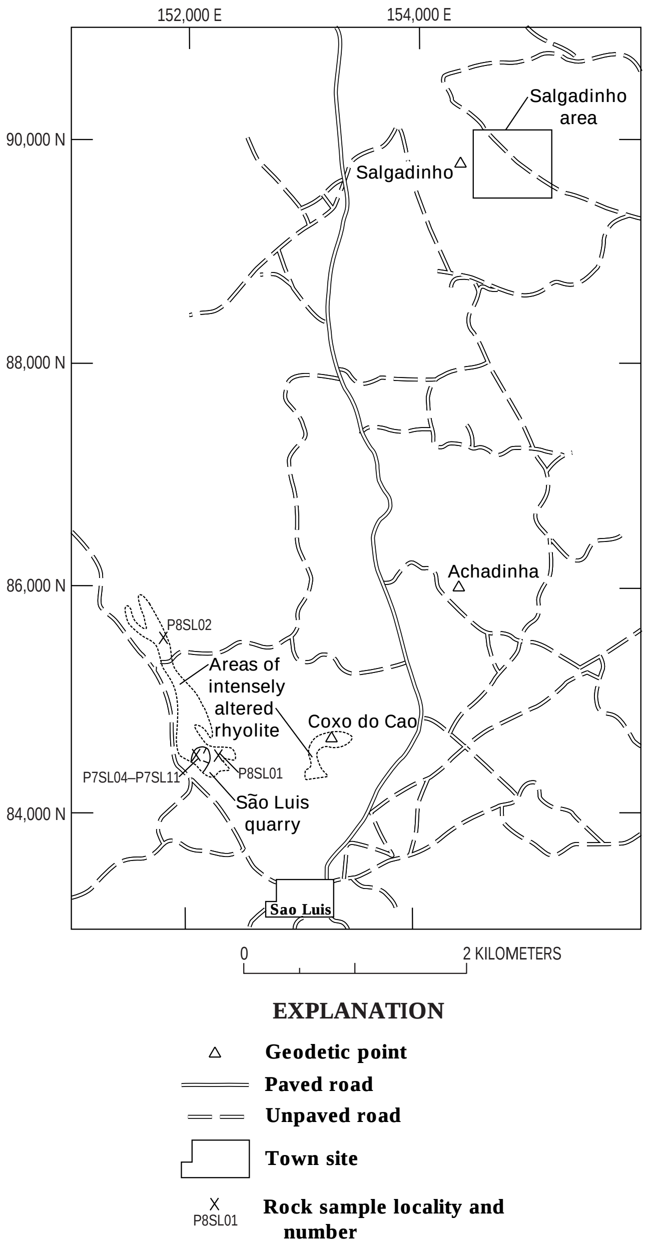

Figure 6. Sketch map showing location of the São Luis-Salgadinho area.

deposit is hosted by felsic volcanic rocks largely of pyroclastic origin with abundant interbeds of fine-grained sedimentary rocks. In contrast to the coarse-textured felsic tuff at Chança, the dominant rock type at Salgadinho is fine-grained pyroclastic beds. Interbedded with the pyroclastic rocks are fine-grained and thinly laminated sedimentary phyllite and tuffite rocks. The felsic volcanic rocks are overlain by the São Luis Shale, forming the top of the VS Complex in this area. The São Luis Shale consists of graphitic shale, tuffite, siliceous shale with local lenses of exhalative cherts in the lower part (Carvalho, 1976; Plimer and Carvalho, 1982). The lithologic and textural characteristics of volcanic and associated rocks confirm the interpretation of a distal setting of the sulfide deposition. The sulfide deposit and the highly deformed host rocks are faulted by both high-angle and low-angle faults and three phases of deformation, F1, F2, and F3 are identified in the region (Plimer and Carvalho, 1982). The most intense phase of deformation is F1, characterized by tight isoclinal folds.

Plimer and Carvalho (1982) determined four alteration types and distributions in the Salgadinho area. In order of decreasing intensity they are (1) green sericite, pyrite, chalcopyrite, quartz, ankerite, and chlorite; (2) green sericite, pyrite, quartz, and chlorite; (3) green sericite and quartz; and (4) green sericite. Plimer and Carvalho identified the green sericite as celadonitic fluoro-muscovite and noted a dramatic increase in fluorine in the more intensely altered zones. An additional alteration type, intense silicification, key to understanding the distribution of gold, was recognized during the present studies.

The Serviço de Fomento Mineiro completed studies in the Salgadinho area in 1982 but the results have not been published. The Salgadinho deposit was drilled to determine the potential for base metals; gold values in individual core samples of disseminated sulfides were as high as 16 g/t. Anomalous gold values were widely scattered and occurred over narrow intervals generally less than 1 m thick. No attempt was made during the earlier studies to determine alteration, lithologic, or geochemical controls with respect to gold distribution.

The present studies, designed to evaluate the distribution of gold with respect to lithologic type, alteration type, and geochemical associations, re-examined drill cores from 8 holes. A total of 135 samples of altered rock were collected from the drill core (pl. 1). The 135 samples which consist of (1) felsic volcanic rocks (46 samples), (2) sedimentary rocks (63 samples), and (3) veins and breccias (26 samples) were analyzed for 34 elements. Analytical results of selected elements in these three sample populations are shown in Appendix A and correlation coefficients are given in table 5. Anomalously high concentrations of gold (as much as 4.8 g/t) were detected in all three of the lithologic categories (App. A). Lithologic and alteration data along with drill hole intersections with significant gold and silver enrichment are shown on plate 1. The samples that contain gold in concentrations of 200 ppb or more occur in the middle and lower parts of the disseminated sulfide body, with the notable exception of sample SL0704, collected from sedimentary rocks in the upper part. Two samples that contain anomalously high gold (SL2609, SL2610), were collected from quartz-sulfide veins in chlorite-rich footwall rocks. In similar deposits in other parts of the world, arsenopyrite is rarely associated with sulfide; however, when it is identified, it is associated with anomalously high concentration of gold (sample SL2809; App. A). Although most gold-bearing zones in the IPB contain ankerite and green sericite in the alteration mineral assemblages, both minerals are common in alteration zones that do not contain anomalous gold. Consequently, ankerite and green sericite are not considered to be indications of potential gold targets in this geologic environment.

Plate 1 shows that gold enrichment in the Salgadinho deposit is widespread and is most common in strongly silicified rocks. There are two types of silicification in the gold-bearing zones: (1) silica flooding, and (2) quartz veins. Silica flooding is most common in the felsic volcanic unit that makes up a major part of the disseminated sulfide host rocks and it consisted of almost total replacement of the rock-forming minerals by SiO_2. In addition, laminated siliceous tuff, chloritic tuff, lapilli tuff, and phyllite and tuffite that are interbedded in the volcanic rocks are locally silica flooded and pyritic, and contain anomalously high gold. Locally anomalous concentrations of gold in quartz veins occur as fracture fillings in both the footwall stringer zone and in fault zones in the disseminated sulfides that are closely associated with fault breccias.

Alteration mineral assemblages and indicator elements that occur with gold are similar in the various lithologic types. The elements, however, that occur with gold in veins and breccias in fault zones in the disseminated sulfides are distinctly different from those in the other rocks (App. A). We believe that gold, originally deposited with disseminated sulfides in the volcanic and sedimentary rocks, may have been preferentially remobilized during deformation into veins and breccias in the disseminated sulfide body. Veins in the footwall stringer zone differ from those in the disseminated sulfide body in that they contain silver-to-gold ratios of less than 1 as opposed to veins in the disseminated sulfide fault zones that contain silver-to-gold ratios of greater than 5. The two vein types are of different ages and origins; those in the footwall are related to disseminated sulfide deposition while those in the disseminated sulfide zone are related to post-mineralization faults. There is no consistent pattern in the fault zone veins between gold and associated elements as determined by chemical analysis. In the Salgadinho area, slump and other gravity slide features indicate that the disseminated sulfide body has, in part, been transported by gravity down the paleoslope. In most places it is detached from the footwall, and consequently underlain only locally by feeder or stringer veins.

In the felsic volcanic rocks, gold has a strong positive geochemical correlation with silver and copper (table 5) and very low or negative correlation coefficients with antimony and zinc. Antimony and zinc are commonly found in the lower temperature minerals formed in upper parts of disseminated or massive sulfide deposits (table 5).

The geologic and geochemical data collected in the Salgadinho area suggest that gold was introduced during the earlier, higher temperature phase of disseminated sulfide deposition and so, by inference, was precipitated from a chloride complex. When precipitated under these conditions, gold occurs primarily in the lattice of the copper sulfide minerals, to a lesser degree in pyrite or as free gold in pyrite, and rarely, such as at the Mt. Morgan, Australia, in telluride minerals (Huston and Large, 1989). Geochemical associations at Salgadinho, similar to those at Chança, have anomalously high concentrations of gold occurring in a greater variety of lithologies. Some gold may have been remobilized preferentially into dilatant structures such as fault zones, during post-mineralization tectonic events.

The distribution of gold in a variety of lithologic types of both volcanic and sedimentary origin suggests an epigenetic origin. Plimer and Carvalho (1982) noted that the disseminated sulfides in the Salgadinho area are hosted by porphyritic felsic volcanic rocks and, although stratabound, they are not of exhalative origin. Gold distribution and geochemical associations determined in our studies would seem to confirm a pore-filling or replacement origin for the gold. An epigenetic origin for the sulfides seems probable; sulfides and gold were deposited very close in time at or near the sea floor. The copper- and gold-bearing hydrothermal solutions were probably associated with sea floor hot spring activity; the solutions permeated the porous underlying felsic tuffaceous volcanic rocks. Sedimentary rocks intercalated in the volcanic rocks commonly have sedimentary flow structures, indicating a steep paleoslope and penecontemporaneous faulting at the time of their formation. Movement of the hydrothermal solutions or their precipitates down the paleoslope could facilitate the concentration of heavy mineral precipitates as suggested by gold concentrations in some turbidite sequences that are synchronous with nearby sulfide deposits of volcanogenic origin.

SÃO DOMINGOS AREA

Gold in the São Domingos area occurs in felsic volcanic rocks in the vicinity of and peripheral to a massive sulfide deposit as well as in exhalite deposits that overlie the deposit. The exhalite deposits are discussed in a later section. Twenty-two felsic volcanic rock samples from the São Domingos area were analyzed for gold and associated elements (App. A). Of these, three (14 percent) contained anomalous concentrations of gold that ranged from 100 to 950 ppb Au. In contrast, 30 andesite and basalt samples contained a maximum concentration of 6 ppb gold and 37 epiclastic rock samples contained less than 6 ppb gold, although several showed the effects of weak sericitic alteration (App. A). All of the anomalous samples were collected within 200 m of the now mined out massive sulfide deposit. Samples from drill hole number MP3, located about 2.5 km west of the massive sulfide body, contain 2 ppb or less gold. The geology and sample localities are shown on plate 2, map A.

GOLD DISTRIBUTION IN CHERT, BEDDED BARITE, AND OTHER ROCKS OF EXHALATIVE ORIGIN

The distribution of gold in rocks of exhalative origin, exclusive of massive sulfides, was the subject of an previous report by the SGP and USGS to the Luso American Development Foundation (Serviços Geológicos de Portugal and U.S. Geological Survey, 1988). The report discusses the distribution of gold in chert and bedded barite samples collected near massive sulfide deposits at Aljustrel in the Portuguese Pyrite Belt. Samples from exhalite massive sulfide deposits exhibited change from barite facies in the proximal setting above the massive sulfide deposits to manganiferous chert facies rocks 1 km or more from the massive sulfides. The distribution of selected elements, including gold, in the barite and chert facies are shown on figure 7.

Rock samples containing barite and chert were collected as part of the study in 1988 in the following areas in the PPB: (1) the southernmost volcanic sub-belt, including the Rosário-Neves-Corvo anticline, near Castro Verde in the area between the Ferragudo manganese mine and the Serpe manganese prospects, and (2) the São Domingos mine area (pl. 2, map A). Additional exhalite samples were collected from the PPB during the present reconnaissance work.

Exhalite deposits of the PPB include chert, jasperoidal chert, quartz-sericite-chlorite-barite rock, massive-bedded barite, and very minor oxide and sulfide facies iron formation. Composition of the exhalites varies with respect to depositional setting relative to volcanic centers. In the following discussion, proximal exhalites are represented by layered sequences that include barite-rich and manganese-poor chemical sediments. Distal exhalites include manganese-rich cherts and related chemical sediments. The proximal to distal facies changes occur over distances of 1 to 7 km. The proximal and distal relationships reflect rapid changes in the depositional environments and are discussed in the previous report (Serviços Geológicos de Portugal and U.S. Geological Survey, 1988).

To further test the distribution of gold in exhalites, a zone across the Rosário-Neves-Corvo anticline was sampled. The area was chosen because (1) it is distant from known massive sulfide occurrences (11 km northwest of deposits at Neves-Corvo) and (2) barite-rich proximal facies rocks are exposed near the core of the anticline and manganese occurs in exhalative cherts on the flanks (fig. 8). Most samples in both proximal and distal settings do not have detectable amounts of gold at the limit of determination (2 ppb) (App. A). In the proximal setting of the Rosário-Neves-Corvo anticline, a maximum concentration of 2 ppb Au was detected in the rock samples (fig. 8). In the distal setting, most samples were found to contain 2 ppb or less gold, although in the northwestern distal facies one sample contains 50 ppb and two samples in the southeastern distal facies contain anomalous gold (29 and 100 ppb). These weakly anomalous amounts of gold in the distal facies are inconclusive, but they support the conclusion at Aljustrel that gold is most highly concentrated in the distal facies (fig. 7).

In the São Domingos area, numerous rock types were sampled for their gold content. The gold distribution in felsic volcanic rocks was previously discussed in the section “Gold in disseminated sulfide deposits, São Domingos area.” Twenty representative samples of exhalites, stratigraphically above the massive sulfide deposit and the felsic volcanic rocks, were collected (App. A). Two of the 20 samples (10 percent) contained ore-grade values of gold (5.5 ppm and 30 ppm) and are located on plate. 2, map A. In contrast to other exhalite localities, the two samples with highly anomalous gold at São Domingos occur in exhalites with anomalously high barite and anomalously low or normal concentrations of manganese; the abundances of these elements are relatively low at São Domingos as compared to exhalites in other parts of the PPB. The rocks that overlie the exhalites at São Domingos consist of epiclastic rocks that commonly have been weakly sericitized. The epiclastic rocks contain a maximum of 6 ppb Au (App. A), which suggests that the gold in the underlying exhalites may have formed at or about the time of deposition of the exhalites or before deposition of the overlying rocks. The exhalative rocks in the São Domingos area consist primarily of green to maroon chert with varying amounts of pyrite. Sample no. P8SD14 contained 30 ppm Au and is green chert with layers or bands of pyrite and minor galena. Analytical results indicate that the anomalous elements associated with gold mineralization include silver, arsenic, antimony, and lead (table 5). The two samples with highly anomalous Au contained abundant pyrite.

Studies of the exhalative rocks in the PPB lead to the following observations related to the distribution of gold: (1) Gold values in proximal or distal exhalite deposits are higher when located in the vicinity of massive sulfide deposits than when more distant from massive sulfides. (2) Where massive sulfide deposits are overlain by barite-rich exhalites (Aljustrel), gold values increase distally toward the manganiferous facies. São Domingos is an exception to this generality. (3) Where massive sulfide deposits are overlain by cherty pyritic exhalites (low barite), highly anomalous amounts of gold may be present in the proximal facies.

Independent studies by Rahder (1990) conducted in the Spanish Pyrite Belt produced results similar to those in Portugal. He has noted that samples with anomalous gold as well as arsenic and antimony are from manganiferous-facies exhalite. He observed that sulfide-bearing jasper-facies contain only normal or background amounts of gold. This observation is consistent with our findings in all of the areas sampled, except São Domingos where sulfide-bearing jasper-facies exhalites contain ore-grade values of gold.

Results from our studies suggest that exhalative rocks should be systematically analyzed for gold and associated elements. The occurrence of highly anomalous gold values

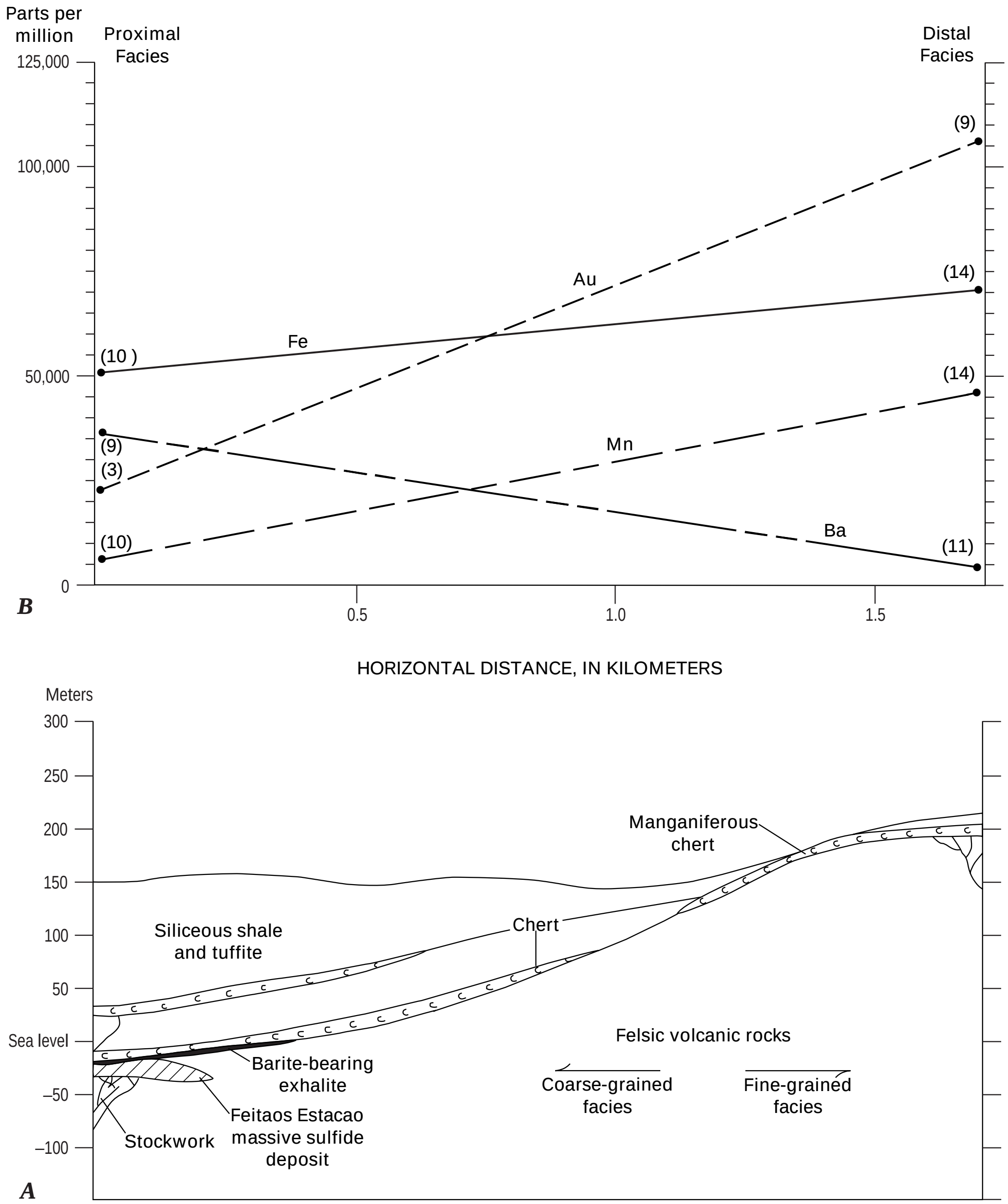

Figure 7. Proximal and distal settings of exhalative chert and baritic rocks at Aljustrel, in the Portuguese Pyrite Belt. *A*, Simplified geologic cross section using a vertical exaggeration ×2. *B*, Distribution trends of selected elements. Values in parts per million: Fe, actual value; Mn, ×10; Ba, ×10; and Au, ×1,000. Numbers in parentheses indicate number of quantified values used in determinations. Note, trends do not necessarily extend beyond parameters of diagram.

in the vicinity of massive sulfide deposits and an absence of highly anomalous gold values in nonmineralized areas suggests that a study of the gold distribution in exhalites may have limited application in the search for buried massive sulfide deposits. Although highly anomalous gold may indicate the presence of a buried massive sulfide deposit, the presence of only background concentrations would not necessarily rule out the presence of massive sulfides; thus, caution should be exercised applying this tool. In the vicinity of a deposit, 90 percent or possibly more of the exhalite samples may contain only background gold concentrations. In the interpretation of the geochemical data, it is important to determine which exhalite facies is present in the area.

The distribution of gold in a massive sulfide deposit may provide clues to the distribution of gold in the overlying exhalite deposits. As discussed in the section “Gold in massive sulfide deposits”, two modes of gold occurrence were recognized in Australia and eastern Canada: (1) gold in the upper zinc-rich parts of massive sulfide deposits and (2) gold in the lower copper-rich parts of massive sulfide bodies and

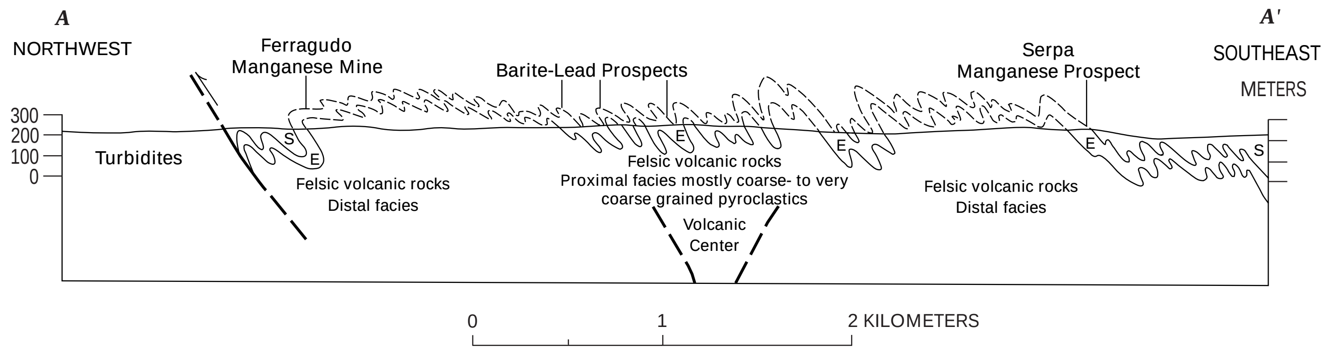

ANALYTICAL RESULTS

NW DISTAL FACIES

SAMP. No.	Au	Ba	Mn	Ag	Cu	Pb	As	DESCRIPTION
P7N16	.002	1000	>5000	N	150	300	N	Chert w/Mn
P7N17	N	20	700	N	10	10	N	Chert-jasper
P7N18	.002	50	1000	<.5	100	150	N	Chert-pyritic
P7N19	.050	1000	>5000	N	300	N	200	Chert-pyritic
P8N29	N	81	>24,000	N	310	N	580	Chert w/Mn
P8N30	N	11	1,100	N	110	190	220	Chert-pyritic
P8N31	<.002	16	7,900	N	180	820	300	Vitric tuff
P8N32	N	31	4,000	N	140	20	180	Siliceous exhalite

DISTAL FACIES SE

SAMP. No.	Au	Ba	Mn	Ag	Cu	Pb	Ag	DESCRIPTION
P7N1	.029	30	700	N	30	15	N	Chert
P7N2	.10	1500	>5000	N	300	N	200	Chert
P7N3	N	30	70	N	7	<10	N	Chert
P7N5	N	200	500	N	10	10	N	Chert

PROXIMAL FACIES

SAMP. No.	Au	Ba	Mn	Ag	Cu	Pb	As	DESCRIPTION
P7N20	N	70	700	N	200	30	N	Chert-pyritic
P7N21	N	500	500	1.5	100	150	N	Chert
P7N22	N	1000	200	N	15	100	N	Chert-pyritic
P8N1	N	>1300	900	N	26	180	16	Altered felsic tuff
P8N3	N	>1300	850	N	1	89	34	Jasper w/Mag
P8N4	<.002	200	720	N	16	140	4	Chert exhalite
P8N5	N	1200	150	N	66	650	16	Bedded barite
P8N6	N	>1300	51	N	11	1900	N	Siliceous exhalite
P8N7	N							Altered felsic tuff
P8N8	N	>1300	20	N	22	64	N	Coarse barite
P8N9	N	>1300	31	N	10	260	7	Siliceous exhalite
P8N10	N	170	190	N	17	220	17	Chert-pyritic
P8N11	N	>1300	210	N	7	170	16	Coarse barite
P8N12	N	>1300	170	N	41	220	5	Siliceous exhalite
P8N13	.002	890	94	4.8	450	2600	75	Siliceous exhalite

Figure 8. Interpretative cross section across Neves-Corvo anticline from the Ferragudo manganese mine to the Serpa manganese prospects; S, shale, siltstone, graywacke, and tuffite; E, chert, barite exhalites, felsic tuff, and black and purple shales. Analytical results of selected elements in parts per million from samples of proximal and distal exhalative rocks collected on or near the line of cross section; N, not detected at lower limit of determination; Mn, manganese; Mag, magnetite.

in the upper part of underlying stringer ore. Gold occurs in most massive sulfide deposits in one of these settings to the exclusion of the other (Huston and Large, 1989); the reason for this difference is poorly understood. Commonly where the exhalites consist of a barite-bearing proximal facies and a manganese-chert distal-facies, anomalously high concentrations of gold are present in the barite facies if gold in the underlying massive sulfide deposit shows a preferential partitioning in the zinc-rich part. As discussed previously, gold in the PPB occurs primarily in the copper-rich parts of the massive and disseminated sulfide deposits. Gold is generally absent in the overlying barite-bearing exhalites, but is locally present in anomalous amounts in the distal exhalite facies which is characterized by high concentrations of manganese.

GOLD DISTRIBUTION IN ULTRAMAFIC AND ASSOCIATED ROCKS OF THE MOBILE BELT

The Mobile Belt is a narrow structurally complex terrane that separates the SPZ to the south from the Ossa-Morena geologic province to the north (figs. 2, 4). The Belt is composed largely of ultramafic rocks and associated rocks of ophiolitic affinity. This sequence of rocks, called the Beja-Acebuches Ophiolite by Munhá and others (1986), crops out at the northern boundary of the Pulo do Lobo Antiform, which is a regional structure in the extreme north of the SPZ at the boundary with the Ossa-Morena Zone. The ophiolite belt, about 1.5 km wide and more than 100 km long along strike, contains rocks characteristic of ophiolite assemblages ranging from serpentinite, gabbro, metagabbro (including granulite), flaser gabbro, and amphibolite at the base to sheeted dike complex and basalt at the top. The ophiolite belt is interpreted to have formed in a back-arc basin as shown in figure 4. It has a steep metamorphic gradient and tectonic inversion as a result of the metamorphic terrane overthrusting rocks of the Ossa-Morena Zone (Castro and others, 1987). The south boundary is displaced by left lateral faults and the ophiolite was locally dismembered by faults during the Hercynian Orogeny. These structural relationships along with age dates from underlying rocks suggest that the Beja-Acebuches ophiolite formed prior to the formation of the Volcanic-Siliceous Complex, the host formation of the volcanogenic sulfide deposits of the SPZ.

The Mobile Belt in an area to the southeast of Ferreira do Alentejo was studied by Paulo Castro of the Serviços Geológicos de Portugal (fig. 9). His studies consisted of supplementary mapping and outcrop sampling in the ultramafic rock terrane with the purpose of establishing the geologic and geochemical relationship of the carbonate- and chrome mica-altered rocks with the serpentinized ultramafic rocks in the area. These rocks were chosen for study because similar rocks, called listwaenites (Buisson and Leblanc, 1986), are host to gold deposits in several different parts of the world including the gold-bearing quartz veins of the Mother Lode in California, USA; the Mother Lode veins are hosted in or near quartz-carbonate-mariposite (chromium muscovite) altered serpentinite. Listwaenites and, associated gold deposits are located along the edges of ultramafic massifs, in high magnesium basalts and in other ultramafic settings where the rocks are serpentinized (Buisson and Leblanc, 1986). The occurrence of relict chromite and the abundance of chromium, nickel, and cobalt in listwaenite is unique to carbonate-altered rocks; these features suggest replacement of the ultramafic rocks as a result of serpentinization.

The rocks in the Mobile Belt are described by Castro in the following way: (1) Layered gabbro consists of alternating layers of olivine-hypersthene gabbro, gabbro, and anorthosite, locally ductily sheared and assumed to be Late Devonian. Pegmatoid differentiations of similar composition are interlayered in the gabbro. Quartz-carbonate rocks occur in the shear zones. (2) Amphibolite, interpreted to be metamorphosed basalt, is foliated, green, fine-grained amphibole-rich rock occurring along the Ferreira-Ficalho Thrust. Petrographic studies suggest that the rock was subjected to lower grade metamorphism (Batista and others, 1976). (3) Granophyre (plagiogranite?) is fine-grained granite that is locally amphibolitic. Results of studies by Fonseca and Ribeiro, (oral commun., 1988) conducted in a contiguous area suggest that the granophyre either was a product of Precambrian magmatism or developed during Late Paleozoic ophiolite formation. (4) Metagabbro, a coarse-grained, gabbroic rock of amphibolite to granulite metamorphic facies, is the equivalent of the basalt in the ophiolite sequence. (5) Serpentinite consists of undifferentiated serpentinized harzburgite, dunite, and troctolite. In most places the serpentinite contains abundant magnetite and is locally talcose. (6) Quartz-carbonate rock (listwaenite) occurs as elongate bodies interpreted to be fracture controlled in contact with serpentinite and in strike-slip fault zones of left lateral movement. The rock is dominantly quartz-ankerite with mariposite nodules in the carbonate, but contains minor late-stage quartz, calcite veinlets, and minor iron sulfide. Compositional variation results in different colored rocks including tan, light green, dark green, red, and various shades of gray. In gabbro and metagabbro shear zones, mariposite or green mica is lacking. Locally white mica, chlorite, and relict chrome spinel occur. Buisson and Leblanc (1986) describe a similar rock as a product of serpentinization. (7) Devonian metasedimentary rocks of the Horta da Torre Formation (Oliveira and others, 1986) consist of siltite, graywacke, and quartzite. They occur south and north of the Ferreira-Ficalho Thrust; to the north, they are strongly sheared and closely associated with serpentinite and quartz-carbonate-altered rocks.

Geochemical studies of the rocks in the Mobile Belt consisted of the collection and analysis of representative samples of serpentinite and the quartz-carbonate altered rock (fig. 9). Twenty-three samples of serpentinite and 31 samples of quartz-carbonate-altered rock were collected and analyzed to determine whether or not they are related, and to evaluate the distribution of gold in the potentially favorable quartz-carbonate (listwaenite) host rock. Analytical results are included in Appendix A.

The range of values of the ultramafic-associated elements chromium, nickel, and cobalt are very similar in the serpentinite and the quartz-carbonate rock, suggesting that the quartz-carbonate rock was formed as a replacement of the ultramafic rock. In addition, the correlation coefficients of nickel with cobalt are almost identical in the two rock types (table 5). The gold and silver contents are extremely low in both rock types. Precious metal values are not shown

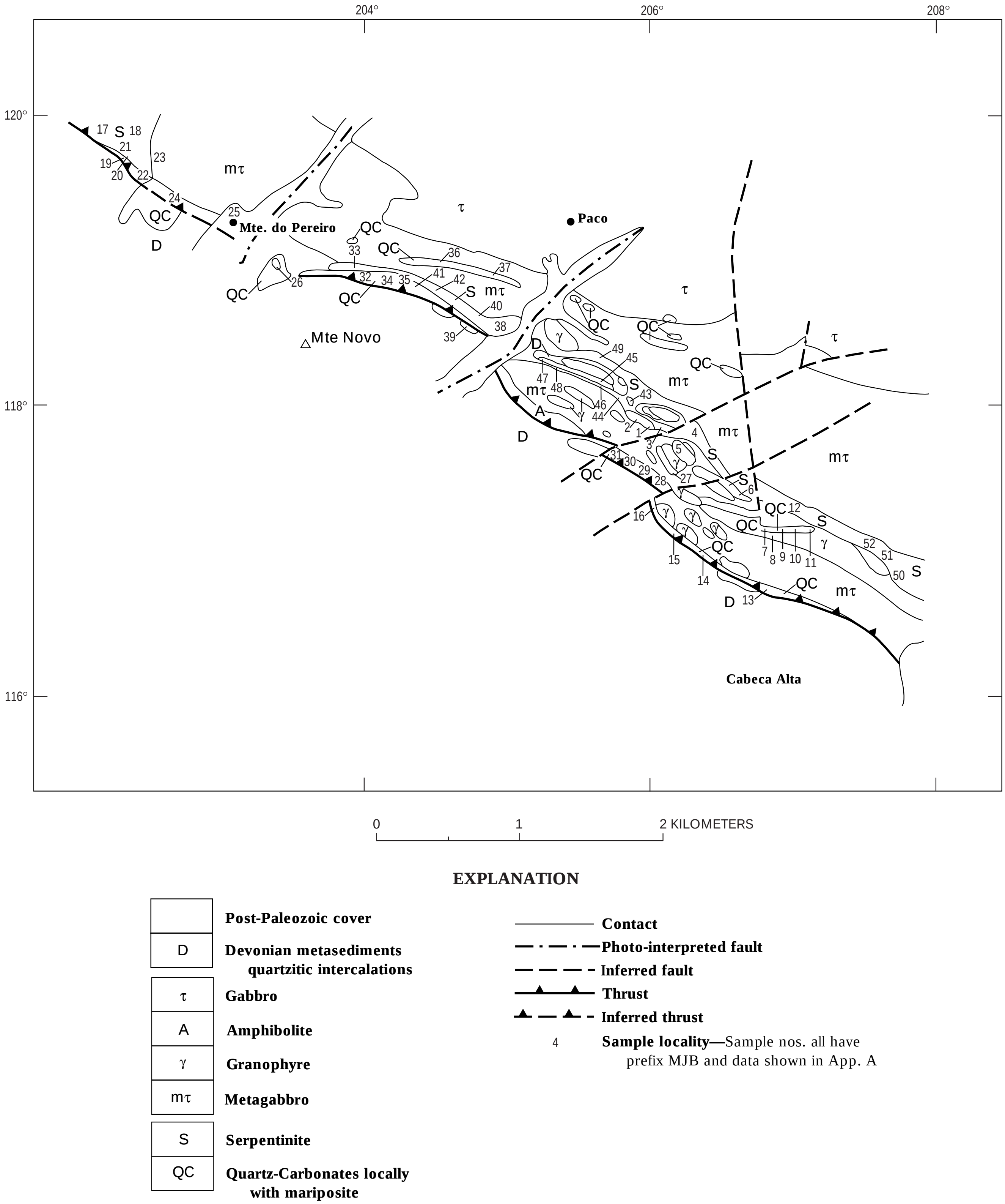

Figure 9. Geology of an area southeast of Ferreira do Alentejo, south Portugal. Modified from Batista and others (1976).

in Appendix A because all samples contained less than the lower limit of detection for gold (2 ppb) and silver (50 ppb). The estimated average crustal abundance of gold in ultramafic rocks is 5 ppb gold (Levinson, 1974); none of the samples analyzed contained as much as 5 ppb gold. The low precious-metal values in the serpentinite might indicate depletion in the serpentinite and enrichment in a nearby environment in which case gold enrichment in the listwaenite would be expected; none of the listwaenite samples, however, contained detectable concentrations of gold and silver. Characteristic features of ultramafic gold host rocks such as development of “late-stage” quartz veins with minor sulfide minerals are lacking in the part of the mobile belt that was studied.

Additional studies of the Beja-Acebuches ophiolite, and particularly the altered serpentinite, are needed to clarify the geology of the area. Geochemical studies of arsenic, barium, boron, antimony, and bismuth may help to delimit zones favorable for precious metals deposits.

GOLD DISTRIBUTION IN OTHER AREAS

Numerous localities in the volcanic sub-belts shown in figure 2 were sampled during general reconnaissance studies. Weakly anomalous gold was found in samples from a few localities characterized by fractured, altered, and mineralized felsic volcanic rocks. Silicification and pyritization are the alteration effects most commonly associated with samples containing anomalous gold.

Samples were collected from the massive sulfide mine areas at Lousal in the eastern part of the PPB, Aljustrel and Juliana in the central part of the PPB, and previously discussed areas at São Domingos and Neves-Corvo. Chemical sediments (exhalites) and altered volcanic rocks are considered to be favorable host rocks for gold deposits in areas with massive sulfide deposits. Epiclastic rocks in the PPB do not appear to be favorable host rocks for gold deposits with the exception of the previously deposit at Salgadinho.

The geology of the Serra Branca area near Corto Gafo (fig. 2) was studied and extensively sampled. In this area, rocks of the VS Complex crop out in the lower plate of a thrust fault that places older rocks of the Phyllite-Quartzite Group (Devonian basement) over the younger Mértola Formation Flysch and VS Complex rocks (pl. 2, map B). A small disseminated sulfide occurrence was mapped in the central part of the area (samples P8SB32-P8SB38); weakly altered to relatively unaltered volcanic rocks occur throughout most of the remaining area. The weakly altered rocks, shown as green alteration zone on cross section *B-B′* (pl. 2) are bleached felsic pyroclastic rocks that commonly contain a greenish mica, particularly along fracture surfaces. Most of the rock samples were collected from the eastern part of the area (pl. 2, map B) and core samples were collected in the western part of the area (cross section *A-A′*, pl. 2). The core samples are primarily varied felsic volcanic and related sedimentary rocks, and were collected to test precious metal contents for a variety of rock and alteration types.

The volcanic sequence consists of several distinctive tuff, agglomerate, and flow units. At the top of the volcanic sequence, chemical sediments and maroon and green shale underlie turbiditic sedimentary rocks of the Mértola Formation. Alteration effects in the eastern part of the area are restricted to the felsic volcanic rocks and are mostly weakly argillized rock with accompanying green mica (sericite?). Rocks are more intensely sericitized or chloritized locally, particularly near fault and shear zones. Silicification alteration is highly localized and rare.

The 48 samples collected from a shear zone that contained vein quartz, calcite, and minor pyrite in the Serra Branca area contained 4 ppb or less gold which is not considered to be significant (App. A). Two core samples collected near the 200-m depth in a drill hole in the western part of the area (*A-A′* on pl. 2, no. SB07) contained 10 ppb and 20 ppb gold, respectively.

Ten samples were collected from intensely altered rhyolitic rocks southwest of the Salgadinho area. The distribution of the altered rocks and sample localities near Sao Luis are shown on figure 6. The altered rhyolite is mostly coarse textured and porphyritic, and is interpreted to be of subvolcanic origin. Argillic, propylitic, potassic, and intense silicic alteration affected the rocks. Propylitic zones contain quartz, epidote, chlorite, and pyrite. Potassic zones are characterized by veins of very coarse pink orthoclase. Narrow quartz veins occupy high-angle fractures in the Sao Luis quarry. An intensely silicified zone, near sample site P8SL01 northeast of the quarry, contained highly anomalous copper (870 ppm), lead (840 ppm), and zinc (greater than 5000 ppm). None of the samples collected in this area of altered rhyolite contained detectable gold.

CONCLUSIONS

Areas in the PPB that contain, or are near, massive sulfide deposits are considered to be most favorable for the discovery of gold deposits. Gold in massive sulfide deposits is most highly concentrated in the copper-rich middle and lower parts of the sulfide deposits and, to a lesser degree, in the underlying footwall rocks. Disseminated sulfide deposits that are hosted by felsic volcanic rocks may also contain highly anomalous gold. Chemical sedimentary rocks that are stratigraphically above several of the massive and disseminated sulfide deposits may also contain anomalous gold; gold appears to be most highly concentrated in distal facies cherts such as at Aljustrel, or in baritic proximal facies cherts such as at São Domingos. Additional areas with potential for gold in the PPB were investigated but do not appear to be promising. These include altered felsic volcanic and subvolcanic rocks that are far removed from massive or disseminated sulfide bodies, and altered ultramafic rocks.

The type of alteration most commonly associated with gold enrichment is silicification which may consist of complete replacement by quartz in the rock-forming minerals or of intrusions of closely spaced quartz veins and stringers. In the PPB, alteration is characterized by carbonate minerals and by sericite, but because these alteration types are widespread they are reliable indicators of gold deposits only where they formed near or in conjunction with intense silicification.

Certain geochemical associations are also useful in the exploration for gold deposits. In the Chança area gold is associated with arsenic, antimony, and copper and in the Salgadinho area, silver and copper appear to be the best gold indicator elements. In exhalative rocks, copper appears to be associated with gold in distal settings and although two samples with highly anomalous gold in proximal exhalite deposits contained highly anomalous silver, arsenic, antimony, and lead, and moderately anomalous bismuth and barium at São Domingos, data are insufficient to assess the potential for gold in exhalite deposits at other proximal settings.

REFERENCES CITED

Baedecker, P.A., and McKown, D.M., 1987, Instrumental neutron activation analysis of geochemical samples, Chapt. H, *in* Baedeker, P.A., ed., Methods for geochemical analysis: U.S. Geological Survey Bulletin 1770, p. H1–H14.

Batista, J.A., Munhá, J., Oliveira, V., and Ribeiro, L., 1976, Alguns aspectos geologico-petrograficos da bordadura sul do Complexo Eruptivo de Beja: Lisbon, Comunicações Serviços Geológicos de Portugal, Tomo LX, p. 203–214.

Buisson, G., and Leblanc, M. 1986, Gold-bearing listwaenites (carbonitized ultramafic rocks) in ophiolite complexes, *in* Gallagher, J.M. Iscer, R.A., Neary, C.R., and Prichard, H.M., eds., Metallogeny of basic and ultrabasic rocks: London, Institute of Mining and Metallurgy, p. 121–132.

Campbell, L.H., Lesher, C.M., Coad, P., Franklin, J.M., Gorton, M.P., and Thurston, P.C., 1984, Rare earth element mobility in alteration pipes below Cu-Zn sulfide deposits: Amsterdam, Elsevier, p. 181–202.

Carvalho, D., 1972, The metallogenic consequences of plate tectonics and the upper Paleozoic evolution of southern Portugal: Estudos Notas Trabalhos Serviço Fomento Mineiro, v. 20, p. 297–320.

———1974, Lineament patterns and hypogene mineralization in Portugal: 4th Symposium, International Association on Genesis of Ore Deposits, Varna, 1974, Problems of ore deposition, v. 2, p. 444–453.

———1976, Considerações sobre do volcanismo da região de Cercal-Odemira, suas relações com a Faixa Piritosa: Lisbon, Comunicações Serviços Geológicos Portugal, Tomo LXII, p 271–315.

———1979, Geologia, Metalogenia e Metodologia da Investigação de Sulfretos Polimetálicos do Sul de Portugal: Lisbon, Comunicações Serviços Geológicos Portugal, no. 65, p. 169–191.

———1991, Case history of the Neves-Corvo massive sulfide deposit, Portugal, and implications for future discoveries, *in* Grauch, R.I., and Hutchinson, R.W., eds., Mineral Deposit Research, Monograph 8 of Economic Geology, Society of Economic Geolologists, Symposium at the Geological Society of America Centennial Meeting, Case Histories of World Class Mineral Discoveries and Historical Perspectives p. 314–334.

Castro, P., Quesada, C., and Munhá, J., 1987, Metamorphic regime in the Beja Acebuches Variscan ophiolite, SW Iberia, Project 233 Report, 1987 Annual Meeting, Mauritania.

Cullers, R. L., and Graf, J. L., 1984a, Rare earth elements in igneous rocks of the continental crust—predominantly basic and ultrabasic rocks, Chapt. 7, *in* Henderson, P., ed., Rare Earth Element Geochemistry: Amsterdam, Elsevier, p. 237–275.

———1984b, Rare earth elements in igneous rocks of the continental crust—intermediate and silicic rocks, ore petrogenesis, Chapt. 8, *in* Henderson, P., ed., Rare Earth Element Geochemistry: Amsterdam, Elsevier, p. 275–317.

Franklin, J.M., Lydon, J.W., and Sangster, D.F., 1981, Volcanic associated massive sulfide deposits, *in* Skinner, B.J., ed., Society of Economic Geology 75th Anniversary Volume: p. 485–627.

Frets, D.C., and Balde, R., 1975, Mount Morgan copper-gold deposit, *in* Knight, C.L. ed., Economic geology of Australia and Papua New Guinea; I, Metals: Australian Institute Mining Metallurgy, Monograph 5, p. 779–785.

Graf, J.L. Jr., 1977, Rare earth elements as hydrothermal tracers during the formation of massive sulfide deposits in volcanic rocks: Economic Geology, v. 72, no. 4, p. 527–548.

Grimes, D.J., and Carvalho, D., 1995, Geochemical exploration studies in the Portuguese Pyrite Belt: U.S. Geological Survey Bulletin 2081–G, p. 53–77.

Grimes, D.J., and Marranzino, A.P., 1968, Direct current arc and alternating-current spark emission spectrographic field methods for the semiquantitative analysis of geologic materials: U.S. Geological Survey Circular 591, 6 p.

Huston, D.L., and Large, R.R., 1989, A chemical model for the concentration of gold in volcanogenic massive sulfide deposits: Amsterdam, Elsevier, Ore Geology Reviews 4, p. 171–200.

Leca, X., Ribiero, A., Oliviera, J.T., Silva, J.B., Albouy,L., Carvalho, P., and Merino, H., 1983, Cadre Geologique des mineralisations de Neves-Corvo, Baixo Alentejo, Portugal: Bureau de Recherches Geologiques et Minieres Memoir 121, 80 p.

Levinson, A.A., 1974, Introduction to exploration geochemistry: Maywood, Ill., Applied Publishing Ltd., p. 43–44.

Lotze, F., 1945, Zur Gleiderung der Varisziden der Iberischen Meseta: Berlin, Geotetonische Forschungen 6, p. 78–92.

Meier, A.L., 1980, Flameless atomic absorption determination of gold in geological materials: Journal of Geochemical Exploration, v. 13, p. 77–85.

Munhá, J., 1979, Blue amphiboles, metamorphic regime and plate tectonic modeling in the Iberian Pyrite Belt: Berlin, Contributions Mineralogy Petrology, v. 69, p. 279–289.

———1983, Hercynian magmatism in the Iberian Pyrite Belt, *in* Lemos De Sousa, M.J., and Oliviera, J.T., eds., The Carboniferous of Portugal: Lisbon, Memorias Serviços Geológicos Portugal 29, p. 39–81.

Munhá, J., Oliviera, J.T., Ribiero, A., Quesada, C., and Kerrick, R., 1986, Beja-Acebuches Ophiolite—Characterization and Geodynamic Significance [abs.]: Maleo, Sociedade Geológica de Portugal, v. 13, no. 2, p. 31.

Motooka, J.M., and Sutley, S.J., 1982, Analysis of oxalic leachates of geologic materials by inductively coupled plasma-atomic-emission spectroscopy: Applied Spectroscopy, v. 36, p. 524–533.

Oliveira, J.T., 1983, The marine Carboniferous of South Portugal—A stratigraphic and sedimentological approach, *in* Lemos de Sousa, M.J., and Oliviera, J.T., eds., The Carboniferous of Portugal: Memórias Serviços Geológicos Portugal 29, p. 3–33.

———1990, Stratigraphy and synsedimentary tectonism, *in* Dottmeyer, R.D., and Martinez Garcia, E., eds., The Mesozoic geology of Iberia: Berlin, Springer-Verlag, p. 335–347.

Oliveira, J.T., Cunha, T.A., Streel, M., and Vanguestaine, M., 1986, Dating the Horta da Torre Formation, a new lithostratigraphic unit of the Ferreira-Ficalho Group, South Portuguese Zone, geological consequences: Communicações Serviços Geológicos Portugal, v. 72, nos. 1–2, p. 129–135.

Plimer, I.R., and Carvalho, D., 1982, The geochemistry of hydrothermal alteration at the Salgadinho copper deposit, Portugal: Berlin, Mineralium Deposita, v. 17, no. 2, p. 193–211.

Rahders, E., 1990, Primary and secondary distribution of gold and silver in host-rocks of volcanogenic massive sulfide deposits in the pyrite belt of Southern Spain [abs.]: 8th International Association on Genesis of Ore Deposits Symposium, Ottawa, p. A280.

Ribeiro, A., Antunes, M.T., Ferreira, M.P., Rocha, R.B., Soares, A.F., Zbyszewski, G., Almeida, F.M., Carvalho, D., and Monteiro, J.H., 1979, Introduction a la Geologia generale du Portugal: Lisbon, Serviços Geológicos de Portugal, Congress International Geology 26E, Paris 1980.

Ribeiro, A., and Silva, J.B., 1983, Structure of the South Portuguese Zone, *in* Lemos de Sousa, M.J., and Oliviera, J.T., eds., The Carboniferous of Portugal: Memórias Serviços Geológicos Portugal 29, p. 83–89.

Sato, J., 1966, On gold bearing ores found in the Shakanai Mine: Hokkaido, Journal Mining Institute, v. 22, p. 1–6.

———1973, A chloride complex model for Kuroko mineralization: Geochemical Journal, v. 7, p. 245–270.

Serviços Geológicos de Portugal and U.S. Geological Survey, 1988, Geologic setting and composition of chert and related rocks in the Portuguese Pyrite Belt—A Preliminary Report: Serviços Geológicos Portugal, Progress Report 1988, 22 p.

Schermerhorn, L.J.G., 1970, The deposition of volcanics and pyritite in the Iberian Pyrite Belt: Berlin, Mineralium Deposita, v. 5, no. 3, p. 273–279.

———1971, An outline stratigraphy of the Iberian Pyrite Belt: Madrid, Boletin Geologico y Minero, v. 82, nos. 3–4, p. 239–268.

———1975, Spilites, regional metamorphism and subduction in the Iberian Pyrite Belt—some comments: Hague, Geologische Bureau voor Het Mijngebied, v. 54, no. 1, p. 23-35.

Strauss, G.K., and Beck, J.S., 1990, Gold mineralization in the southwestern Iberian Pyrite Belt: Berlin, Mineralium Deposita, v. 25, p. 237–245.

Published in the Central Region, Denver, Colorado
Manuscript approved for publication December 17, 1997
Graphics prepared by Norma J. Maes and Mike Kirtley
Photocomposition by Norma J. Maes

APPENDIX

Appendix A. Analytical results for selected elements in rocks from the Portuguese Pyrite Belt.

[L, less than limit of determination; N, not detected at the lower limit of determination]

1. CHANÇA AREA—ALL ROCK TYPES

Sample No.	Ag	As	Au	Bi	Cu	Mo	Pb	Sb	Zn
BH301	N0.025	44.0	N0.002	N1.0	2.7	1.0	N1.0	N1.0	23
BH302	N0.025	5.3	N0.002	N1.0	40.0	1.0	N1.0	N1.0	36
BH303	N0.025	N1.0	N0.002	N1.0	24.0	1.0	6.4	N1.0	74
BH304	N0.025	33.0	N0.002	N1.0	15.0	1.0	N1.0	N1.0	10
BH305	N0.025	23.0	0.008	9.9	12.0	1.0	14.0	N1.0	12
BH306	N0.025	29.0	L0.002	6.9	11.0	1.0	13.0	N1.0	28
BH307	N0.025	52.0	0.004	N1.0	20.0	1.0	26.0	N1.0	200
BH308	N0.025	52.0	N0.002	N1.0	6.3	1.0	17.0	N1.0	140
BH309	N0.025	52.0	0.014	N1.0	21.0	1.0	39.0	N1.0	23
BH310	0.047	35.0	0.006	7.3	17.0	1.0	19.0	N1.0	19
BH311	N0.025	24.0	0.006	N1.0	12.0	1.0	25.0	N1.0	86
BH312	N0.025	140.0	0.002	N1.0	9.2	1.0	91.0	N1.0	64
BH313	N0.025	23.0	N0.002	10.0	39.0	1.0	51.0	N1.0	86
BH314	7.800	160.0	0.004	12.0	320.0	1.9	150.0	64.0	290
BH315	1.200	43.0	0.002	11.0	12.0	1.0	20.0	7.9	15
BH316	0.570	31.0	L0.002	7.9	23.0	1.0	16.0	N1.0	23
BH317	N0.025	38.0	N0.002	N1.0	3.5	1.0	10.0	N1.0	30
BH318	N0.025	31.0	N0.002	N1.0	31.0	8.7	18.0	N1.0	11
CH101	N0.025	36.0	N0.002	N1.0	17.0	N1.0	N1.0	1.0	23
CH102	N0.025	N1.0	L0.002	N1.0	7.7	N1.0	N1.0	1.0	36
CH103	N0.025	N1.0	0.004	N1.0	2.7	N1.0	6.9	1.0	32
CH104	N0.025	39.0	L0.002	N1.0	12.0	N1.0	15.0	1.0	54
CH105	N0.025	57.0	L0.002	6.2	9.9	N1.0	13.0	1.0	30
CH106	N0.025	26.0	N0.002	7.7	12.0	N1.0	23.0	1.0	37
CH107	N0.025	32.0	0.004	6.8	17.0	N1.0	16.0	1.0	23
CH108	N0.025	95.0	L0.002	N1.0	35.0	N1.0	49.0	1.0	140
CH109	N0.025	500.0	0.150	N1.0	2000.0	N1.0	54.0	1.0	N1
CH110	N0.025	100.0	0.044	18.0	5000.0	N1.0	20.0	1.0	57
CH111	N0.025	350.0	0.200	N1.0	2000.0	27.0	90.0	67.0	N1
CH112	N0.025	37.0	0.048	N1.0	88.0	N1.0	68.0	1.0	73
CH113	N0.025	N1.0	L0.002	N1.0	6.8	N1.0	9.3	1.0	66
P8CH01	N0.025	15.0	L0.002	N1.0	17.0	N1.0	7.4	N1.0	7
P8CH02	N0.025	20.0	N0.002	N1.0	4.1	N1.0	N1.0	N1.0	11
P8CH03	N0.025	30.0	L0.002	N1.0	8.9	50.0	N1.0	N1.0	63
P8CH04	N0.025	19.0	N0.002	N1.0	9.2	N1.0	6.6	N1.0	49
P8CH05	N0.025	220.0	0.050	N1.0	160.0	L1.0	23.0	N1.0	41
P8CH06	1.500	34.0	0.006	N1.0	4.9	1.3	46.0	N1.0	8
P8CH07	N0.025	34.0	L0.002	N1.0	33.0	N1.0	24.0	N1.0	77
P8CH08	N0.025	5.3	N0.002	N1.0	12.0	N1.0	11.0	N1.0	85
P8CH09	N0.025	89.0	0.046	N1.0	75.0	N1.0	N1.0	N1.0	41
P8CH10	N0.025	110.0	0.012	N1.0	160.0	N1.0	N1.0	N1.0	61
P8CH11	N0.025	8.6	N0.002	N1.0	4.4	N1.0	N1.0	N1.0	24
P8CH12	N0.025	N1.0	N0.002	N1.0	29.0	N1.0	N1.0	N1.0	89
P8CH13	N0.025	N1.0	0.016	N1.0	1.0	N1.0	N1.0	N1.0	5
P8CH14	N0.025	41.0	0.002	N1.0	74.0	N1.0	5.4	N1.0	18
P8CH15	N0.025	300.0	0.010	N1.0	110.0	3.1	15.0	N1.0	13
P8CH16	N0.025	89.0	0.020	N1.0	2.1	N1.0	48.0	N1.0	15

P8CH17	N0.025	94.0	0.006	N1.0	97.0	N1.0	43.0	N1.0	13
P8CH18	N0.025	8.8	N0.002	N1.0	5.2	N1.0	18.0	N1.0	40
P8CH19	N0.025	28.0	N0.002	N1.0	21.0	N1.0	10.0	N1.0	53
P8CH20	N0.025	20.0	N0.002	N1.0	17.0	N1.0	5.4	N1.0	31

2. SALGADINHO AREA—EPICLASTIC ROCKS

Sample No.	Ag	As	Au	Bi	Cu	Pb	Zn
SL0502	N0.025	17.0	L0.002	N1.0	28.0	32.0	75
SL0503	N0.025	15.0	L0.002	N1.0	12.0	11.0	77
SL0513	N0.025	15.0	N0.002	N1.0	4.7	13.0	26
SL0516	N0.025	7.6	0.004	7.0	29.0	12.0	77
SL0518	N0.025	13.0	0.050	N1.0	410.0	16.0	71
SL0521	1.800	26.0	4.800	N1.0	1200.0	38.0	97
SL0523	23.000	92.0	0.150	110.0	8300.0	570.0	440
SL0524	11.000	42.0	0.018	68.0	8600.0	57.0	66
SL0702	N0.025	23.0	L0.002	N1.0	37.0	7.4	46
SL0713	N0.025	25.0	N0.002	N1.0	15.0	13.0	55
SL0704	55.000	69.0	2.700	210.0	2000.0	1700.0	1800
SL0706	N0.025	24.0	0.002	6.9	20.0	27.0	98
SL0707	N0.025	16.0	N0.002	N1.0	20.0	16.0	62
SL1501	N0.025	10.0	0.002	N1.0	5.2	160.0	73
SL1502	N0.025	29.0	0.010	11.0	5.1	10.0	64
SL1503	N0.025	25.0	N0.002	N1.0	2.3	N1.0	55
SL1504	1.500	22.0	0.008	8.1	2600.0	6.0	190
SL1505	N0.025	9.9	0.004	6.0	2.5	1.0	35
SL1513	N0.025	20.0	L0.002	6.3	15.0	93.0	420
SL1514	5.800	16.0	0.150	21.0	230.0	260.0	69
SL1901	N0.025	23.0	0.002	N1.0	26.0	N1.0	65
SL1902	N0.025	9.5	N0.002	N1.0	12.0	N1.0	41
SL1903	N0.025	11.0	N0.002	N1.0	31.0	36.0	68
SL1904	N0.025	18.0	L0.002	N1.0	37.0	110.0	110
SL1905	N0.025	18.0	L0.002	N1.0	16.0	20.0	76
SL1906	1.200	54.0	0.022	N1.0	34.0	1300.0	2400
SL1907	N0.025	47.0	0.012	N1.0	48.0	200.0	130
SL1908	N0.025	25.0	0.006	N1.0	39.0	51.0	130
SL1913	N0.025	5.5	0.004	N1.0	4.8	1.0	36
SL1914	N0.025	23.0	0.040	N1.0	4.5	10.0	59
SL1916	N0.025	45.0	0.008	N1.0	21.0	40.0	59
SL1917	N0.025	30.0	0.004	7.2	3.4	440.0	1300
SL1918	N0.025	16.0	L0.002	8.6	8.0	56.0	30
SL2101	N0.025	7.0	0.002	8.6	6.9	7.6	95
SL2104	N0.025	14.0	L0.002	N1.0	4.5	5.2	60
SL2105	N0.025	38.0	0.008	N1.0	48.0	23.0	73
SL2401	1.200	44.0	0.006	N1.0	13.0	430.0	370
SL2402	N0.025	35.0	0.002	N1.0	16.0	320.0	1600
SL2411	N0.025	59.0	0.002	N1.0	35.0	16.0	19
SL2412	N0.025	63.0	0.014	N1.0	13.0	17.0	65
SL2413	N0.025	21.0	N0.002	N1.0	2.9	6.2	50
SL2414	N0.025	35.0	0.150	N1.0	36.0	73.0	89
SL2415	N0.025	36.0	0.008	N1.0	34.0	19.0	58
SL2601	N0.025	33.0	0.004	N1.0	22.0	9.1	76
SL2608	N0.025	20.0	N0.002	N1.0	38.0	7.3	76
SL2611	N0.025	67.0	0.004	N1.0	9.1	300.0	64
SL2612	N0.025	23.0	N0.002	N1.0	64.0	76.0	88

SL2802	N0.025	N1.0	N0.002	N1.0	6.1	14.0	74
SL2803	N0.025	27.0	N0.002	N1.0	17.0	9.6	79
SL2804	N0.025	23.0	N0.002	N1.0	23.0	24.0	85
SL2805	N0.025	14.0	N0.002	N1.0	5.2	18.0	320
SL2806	N0.025	N1.0	N0.002	N1.0	0.9	N1.0	36
SL2807	N0.025	19.0	L0.002	N1.0	59.0	N1.0	49
SL2808	N0.025	21.0	L0.002	N1.0	31.0	51.0	100
SL2809	N0.025	14000.0	0.600	N1.0	970.0	250.0	2400
SL2810	N0.025	N1.0	L0.002	N1.0	12.0	N1.0	55
SL2811	N0.025	60.0	L0.002	N1.0	4.7	10.0	80
SL2813	N0.025	41.0	L0.002	N1.0	28.0	33.0	100
SL2815	N0.025	88.0	N0.002	N1.0	6.6	N1.0	31
SL2817	11.000	130.0	0.250	N1.0	2000.0	83.0	N1
SL2818	0.570	14.0	0.150	N1.0	1100.0	11.0	39
SL2819	N0.025	41.0	0.002	N1.0	36.0	N1.0	95
SL2821	88.000	830.0	1.400	150.0	2000.0	5.7	N1

3. SALGADINHO AREA—FELSIC VOLCANIC ROCKS

Sample No.	Ag	As	Au	Bi	Cu	Mo	Pb	Zn
P8SA1	N0.025	370.0	0.028	N1.0	80.0	N1.0	N1.0	1500
P8SA2	0.560	21.0	0.002	15.0	84.0	14.0	60.0	580
P8SA3	N0.025	36.0	L0.002	N1.0	55.0	N1.0	N1.0	510
SL0506	N0.025	N1.0	0.002	N1.0	2.6	N1.0	9.9	17
SL0510	N0.025	17.0	L0.002	N1.0	8.0	N1.0	11.0	48
SL0511	N0.025	41.0	0.006	N1.0	16.0	N1.0	35.0	69
SL0512	N0.025	25.0	L0.002	N1.0	17.0	N1.0	27.0	92
SL0519	4.500	36.0	0.038	N1.0	2000.0	1.3	110.0	2400
SL0520	N0.025	24.0	0.018	7.4	220.0	2.5	11.0	24
SL0710	N0.025	19.0	N0.002	6.9	20.0	1.6	21.0	84
SL0711	N0.025	6.2	N0.002	8.0	5.7	N1.0	7.6	52
SL0712	N0.025	N1.0	N0.002	N1.0	11.0	N1.0	N1.0	67
SL0713	N0.025	N1.0	N0.002	11.0	12.0	1.1	34.0	27
SL0714	N0.025	28.0	N0.002	11.0	11.0	2.3	27.0	60
SL1506	N0.025	16.0	0.002	8.6	11.0	2.2	8.4	130
SL1509	N0.025	32.0	0.200	6.2	29.0	N1.0	7.8	69
SL1516	N0.025	23.0	N0.002	6.0	17.0	N1.0	400.0	200
SL1518	N0.025	15.0	N0.002	N1.0	6.5	N1.0	130.0	110
SL1519	N0.025	15.0	N0.002	6.9	36.0	N1.0	14.0	72
SL1919	N0.025	23.0	0.002	7.1	24.0	N1.0	36.0	68
SL1919A	N0.025	48.0	0.004	N1.0	11.0	N1.0	35.0	59
SL2102	N0.025	28.0	0.018	9.9	51.0	3.0	41.0	160
SL2103	N0.025	4.6	0.002	9.6	46.0	N1.0	11.0	49
SL2405	N0.025	160.0	0.012	N1.0	130.0	N1.0	560.0	530
SL2406	11.000	19.0	1.600	N1.0	4000.0	N1.0	150.0	N1
SL2407	4.600	53.0	0.100	N1.0	4000.0	N1.0	68.0	620
SL2408	2.300	54.0	0.250	N1.0	2300.0	N1.0	150.0	75
SL2409	0.920	88.0	0.032	N1.0	2300.0	N1.0	23.0	29
SL2605	N0.025	15.0	0.002	N1.0	170.0	N1.0	21.0	29
SL2606	N0.025	100.0	0.034	N1.0	330.0	N1.0	75.0	25
SL2607	3.400	170.0	0.300	N1.0	1200.0	N1.0	200.0	46
SL2812	N0.025	41.0	0.025	N1.0	180.0	N1.0	39.0	40
SL2822	N0.025	18.0	N0.002	N1.0	20.0	N1.0	5.7	82
SL1517	N0.025	8.7	N0.002	6.8	14.0	N1.0	380.0	110
SL0522	N0.025	23.0	0.004	N1.0	22.0	N1.0	13.0	41

SL0701	N0.025	36.0	L0.002	6.9	66.0	N1.0	110.0	110
SL0705	N0.025	11.0	N0.002	N1.0	19.0	N1.0	17.0	76
SL0707	N0.025	16.0	N0.002	N1.0	20.0	N1.0	16.0	62
SL1909	N0.025	10.0	L0.002	N1.0	10.0	N1.0	14.0	900
SL1910	N0.025	28.0	0.002	N1.0	9.2	N1.0	1.0	87
SL1911	N0.025	59.0	0.004	N1.0	16.0	N1.0	28.0	91
SL1912	1.900	160.0	0.100	N1.0	2600.0	N1.0	44.0	1400
SL2410	5.000	85.0	2.000	N1.0	4000.0	N1.0	24.0	N1
SL2602	N0.025	23.0	0.004	N1.0	41.0	N1.0	19.0	160
SL2603	N0.025	20.0	L0.002	N1.0	43.0	N1.0	55.0	39
SL2604	N0.025	15.0	N0.002	N1.0	19.0	N1.0	1.0	52

4. SALGADINHO AREA—VEINS AND BRECCIAS

Sample No.	Ag	As	Au	Bi	Cu	Pb	Sb	Zn
SL0301	7.000	33.0	0.016	51.0	8300.0	50.0	20	62
SL0501	N0.025	55.0	0.008	N1.0	21.0	20.0	N1	31
SL0504	N0.025	15.0	N0.002	N1.0	15.0	66.0	N1	76
SL0505	N0.025	3.5	N0.002	N1.0	27.0	62.0	N1	150
SL0508	N0.025	36.0	0.006	N1.0	51.0	5.2	N1	58
SL0509	N0.025	16.0	0.004	6.1	3.7	17.0	N1	30
SL0514	N0.025	56.0	0.032	N1.0	150.0	90.0	N1	410
SL0515	2.900	65.0	0.250	15.0	3300.0	87.0	N1	370
SL0517	1.200	47.0	1.300	9.5	1300.0	47.0	N1	130
SL0524	11.000	42.0	0.018	68.0	8600.0	57.0	40	66
SL0709	0.500	27.0	0.002	11.0	19.0	21.0	N1	66
SL1507	N0.025	35.0	0.030	N1.0	33.0	N1.0	N1	94
SL1508	N0.025	49.0	L0.002	N1.0	8.1	N1.0	N1	42
SL1509	N0.025	32.0	0.200	6.2	29.0	7.8	N1	69
SL1510	N0.025	21.0	L0.002	N1.0	23.0	12.0	N1	71
SL1511	N0.025	25.0	L0.002	N1.0	39.0	18.0	N1	55
SL1512	2.900	18.0	0.020	14.0	2800.0	98.0	N1	490
SL1515	N0.025	13.0	L0.002	6.0	46.0	14.0	N1	90
SL1915	2.400	17.0	0.044	21.0	18.0	38.0	N1	69
SL2404	N0.025	21.0	0.002	N1.0	180.0	140.0	N1	420
SL2609	N0.025	22.0	0.100	N1.0	58.0	N1.0	N1	44
SL2610	N0.025	15.0	0.900	N1.0	1000.0	N1.0	N1	110
SL2801	N0.025	27.0	N0.002	N1.0	10.0	36.0	N1	130
SL2814	N0.025	230.0	0.100	N1.0	N1.0	N1.0	N1	110
SL2816	N0.025	73.0	L0.002	N1.0	41.0	7.4	N1	43
SL2823	N0.025	5.9	N0.002	N1.0	21.0	12.0	N1	94

5. SÃO DOMINGOS AREA—FELSIC VOLCANIC ROCKS

Sample No.	Ag	As	Au	Bi	Cu	Mo	Pb	Sb	Zn
MP303	N0.025	N1.0	N0.002	N1.0	0.9	N1	5.9	N1.0	4
MP304	N0.025	N1.0	N0.002	N1.0	0.8	N1	5.5	N1.0	N1
MP316	N0.025	19.0	N0.002	N1.0	9.3	N1	12.0	N1.0	41
MP317	N0.025	N1.0	N0.002	N1.0	3.4	N1	26.0	N1.0	6
MP318	N0.025	N1.0	N0.002	N1.0	1.4	N1	N1.0	N1.0	2
MP319	N0.025	3.5	N0.002	N1.0	3.3	N1	23.0	N1.0	6
MP320	N0.025	3.4	N0.002	N1.0	4.3	N1	19.0	N1.0	19
MP321	N0.025	12.0	N0.002	N1.0	26.0	N1	18.0	N1.0	71
MP322	N0.025	N1.0	N0.002	N1.0	1.4	N1	N1.0	N1.0	29
MP323	N0.025	N1.0	N0.002	N1.0	2.8	N1	N1.0	N1.0	23
MP324	N0.025	N1.0	N0.002	N1.0	1.6	N1	13.0	N1.0	25

MP325	N0.025	6.4	N0.002	N1.0	2.1	N1	9.7	N1.0	35
MP326	N0.025	N1.0	N0.002	N1.0	8.0	N1	N1.0	N1.0	100
MP327	N0.025	N1.0	N0.002	N1.0	14.0	N1	N1.0	N1.0	69
P8SD10	4.300	120.0	0.100	6.7	140.0	N1	920.0	N1.0	8
P8SD11	N0.025	34.0	L0.002	N1.0	29.0	N1	12.0	5.6	2
P8SD12	0.470	140.0	0.012	N1.0	81.0	N1	24.0	N1.0	14
P8SD13	N0.025	170.0	L0.002	N1.0	57.0	N1	87.0	N1.0	5
P8SD15	N0.025	190.0	0.004	N1.0	170.0	N1	67.0	N1.0	13
P8SD45	N0.025	5.6	0.006	N1.0	5.6	N1	23.0	N1.0	13
P8SD46A	N0.025	160.0	0.950	N1.0	18.0	50	15.0	N1.0	12
P8SD47	N0.025	3.3	0.200	8.6	5.7	N1	7.3	N1.0	25

6. SÃO DOMINGOS AREA—INTERMEDIATE TO BASIC VOLCANIC ROCKS

Sample No.	Ag	As	Au	Cu	Pb	Sb	Zn
MSD103	N0.025	N1.0	L0.002	16.0	N1.0	N1.0	1500
MSD104	N0.025	N1.0	L0.002	5.6	N1.0	N1.0	1200
MSD105	N0.025	N1.0	N0.002	5.6	N1.0	N1.0	1100
MSD106	N0.025	11.0	N0.002	1.5	7.4	N1.0	2400
MSD107	N0.025	N1.0	N0.002	1.0	N1.0	N1.0	2400
MSD108	N0.025	5.5	N0.002	2.0	N1.0	N1.0	160
MSD109	N0.025	N1.0	N0.002	300.0	N1.0	N1.0	62
MSD110	N0.025	4.2	0.006	23.0	N1.0	N1.0	120
MSD111	N0.025	N1.0	0.004	29.0	N1.0	N1.0	110
MSD112	N0.025	3.0	N0.002	26.0	N1.0	N1.0	75
MSD113	N0.025	25.0	L0.002	40.0	N1.0	N1.0	150
MSD114	N0.025	N1.0	N0.002	33.0	N1.0	N1.0	120
MSD115	N0.025	N1.0	N0.002	17.0	N1.0	N1.0	89
MSD116	N0.025	N1.0	N0.002	11.0	N1.0	N1.0	110
MSD117	N0.025	N1.0	N0.002	54.0	N1.0	N1.0	140
MSD118	N0.025	N1.0	N0.002	7.3	N1.0	N1.0	120
MSD119	N0.025	N1.0	N0.002	9.7	N1.0	N1.0	87
MSD120	N0.025	N1.0	L0.002	9.4	5.1	N1.0	110
MSD121	N0.025	N1.0	N0.002	26.0	N1.0	N1.0	100
MSD122	N0.025	N1.0	N0.002	15.0	N1.0	N1.0	110
MSD123	N0.025	17.0	0.002	2600.0	N1.0	N1.0	75
MSD124	N0.025	66.0	N0.002	24.0	N1.0	N1.0	54
P8SD16	N0.025	22.0	N0.002	38.0	130.0	N1.0	280
P8SD17	N0.025	41.0	L0.002	64.0	58.0	N1.0	240
P8SD18	N0.025	N1.0	N0.002	26.0	600.0	N1.0	670
P8SD29	N0.025	N1.0	L0.002	28.0	26.0	N1.0	2400
P8SD30	N0.025	35.0	L0.002	210.0	53.0	N1.0	200
P8SD34	N0.025	160.0	L0.002	61.0	34.0	N1.0	30
P8SD35	N0.025	120.0	0.002	30.0	28.0	N1.0	21
P8SD36	N0.025	600.0	0.004	30.0	170.0	9.8	43

7. SÃO DOMINGOS AREA—EPICLASTIC ROCKS

Sample No.	Ag	As	Au	Ba	Bi	Cu	Mo	Pb	Zn
P8SD19	N0.025	10.0	0.004	31	N1.0	98.0	N1.0	21.0	470
P8SD20	N0.025	N1.0	L0.002	38	N1.0	70.0	N1.0	6.4	410
P8SD21	N0.025	61.0	0.002	19	N1.0	180.0	N1.0	34.0	85
P8SD22	N0.025	16.0	0.002	34	N1.0	58.0	N1.0	15.0	930
P8SD23	N0.025	17.0	N0.002	24	N1.0	100.0	N1.0	8.9	810
P8SD24	N0.025	18.0	N0.002	19	N1.0	83.0	N1.0	N1.0	77

P8SD25	N0.025	900.0	N0.002	10	N1.0	160.0	N1.0	N1.0	640
P8SD26	N0.025	14.0	L0.002	15	N1.0	85.0	N1.0	7.8	35
P8SD27	N0.025	150.0	L0.002	10	N1.0	360.0	N1.0	24.0	280
P8SD28	N0.025	38.0	L0.002	17	N1.0	70.0	N1.0	10.0	22
P8SD31	N0.025	N1.0	N0.002	9	N1.0	1100.0	N1.0	N1.0	2400
P8SD32	N0.025	45.0	0.002	10	N1.0	470.0	9.1	25.0	22
P8SD33	N0.025	600.0	N0.002	170	N1.0	29.0	N1.0	260.0	15
P8SD37	N0.025	210.0	0.004	18	N1.0	72.0	N1.0	8.7	1200
P8SD38	N0.025	40.0	N0.002	6	N1.0	88.0	2.1	13.0	140
P8SD39	N0.025	5.6	N0.002	25	N1.0	19.6	N1.0	32.0	320
P8SD40	N0.025	6.6	L0.002	34	N1.0	13.0	N1.0	23.0	380
P8SD41	N0.025	4.6	N0.002	23	N1.0	5.6	N1.0	27.0	950
P8SD42	N0.025	4.0	L0.002	15	N1.0	6.1	N1.0	24.0	930
P8SD43	N0.025	15.0	N0.002	17	N1.0	15.0	N1.0	13.0	300
P8SD06	0.640	45.0	L0.002	12	12.0	1900.0	N1.0	8.3	30
P8SD07	N0.025	140.0	N0.002	11	N1.0	510.0	N1.0	7.3	32
P8SD08	N0.025	2400.0	N0.002	9	N1.0	1400.0	N1.0	N1.0	97
P8SD09	N0.025	9.8	N0.002	13	7.1	40.0	N1.0	8.7	91
MP301	N0.025	N1.0	L0.002	15	N1.0	15.0	N1.0	N1.0	11
MP302	N0.025	7.0	N0.002	21	N1.0	35.0	N1.0	9.1	32
MSD101	N0.025	15.0	0.006	36	N1.0	56.0	N1.0	7.8	510
MSD102	N0.025	65.0	0.006	36	N1.0	120.0	1.7	78.0	180
MSD125	N0.025	6.9	L0.002	34	N1.0	31.0	N1.0	N1.0	61
MSD126	N0.025	N1.0	L0.002	29	N1.0	3.0	N1.0	N1.0	32
MSD127	N0.025	3.2	N0.002	24	N1.0	5.7	N1.0	N1.0	40
MSD128	N0.025	3.1	0.002	26	N1.0	2.4	N1.0	N1.0	23
MSD129	N0.025	25.0	N0.002	19	N1.0	5.3	15.0	8.1	23
MSD130	N0.025	7.1	L0.002	61	N1.0	33.0	N1.0	38.0	45
MSD131	N0.025	11.0	L0.002	32	N1.0	11.0	N1.0	7.1	35
P8SD04	0.530	24.0	N0.002	28	7.3	78.0	N1.0	9.9	16
P8SD05	N0.025	33.0	N0.002	18	N1.0	150.0	N1.0	5.5	80

8. SÃO DOMINGOS AREA—CHEMICAL SEDIMENTS (EXHALITES)

S. No.	Ag	As	Au	Ba	Bi	Cu	Mn	Mo	Pb	SbZn
MP305	N0.025	N1.0	N0.002	21	N1	2.1	57	N1.0	18.0	N12
MP305a	N0.025	3.9	N0.002	21	N1	3.2	670	N1.0	11.0	N12
MP306	N0.025	3.3	N0.002	25	N1	2.4	140	N1.0	8.5	N12
MP307	N0.025	N1.0	N0.002	23	N1	2.9	62	N1.0	12.0	N14
MP308	N0.025	8.7	N0.002	25	N1	1.4	34	N1.0	17.0	N19
MP309	N0.025	29.0	N0.002	18	N1	28.0	280	N1.0	66.0	N139
MP310	N0.025	N1.0	N0.002	15	N1	5.9	46	N1.0	7.4	N15
MP311	N0.025	N1.0	N0.002	23	N1	2.8	30	N1.0	23.0	N15
MP312	N0.025	N1.0	N0.002	16	N1	1.8	46	N1.0	N1.0	N12
MP313	N0.025	N1.0	N0.002	18	N1	1.6	110	N1.0	24.0	N16
MP314	N0.025	3.5	N0.002	11	N1	3.8	35	N1.0	6.6	N15
MP315	N0.025	N1.0	N0.002	17	N1	2.0	73	N1.0	16.0	N16
MP328	N0.025	N1.0	N0.002	25	N1	7.3	690	N1.0	N1.0	N1120
MP329	N0.025	N1.0	N0.002	10	N1	3.6	190	N1.0	N1.0	N125
MP330	N0.025	N1.0	N0.002	13	N1	11.0	600	N1.0	N1.0	N167
P8SD1	N0.025	110.0	0.006	190	N1	820.0	120	N1.0	82.0	N189
P8SD2	N0.025	340.0	0.010	44	N1	790.0	95	N1.0	110.0	N197
P8SD3	N0.025	1200.0	N0.002	16	N1	680.0	76	N1.0	46.0	N193
P8SD14	73.000	940.0	30.000	110	43	40.0	57	2.4	2300.0	8811
P8SD44	4.000	970.0	5.500	120	6	35.0	28	2.2	2400.0	2412

9. CHEMICAL SEDIMENTS (EXHALITES)—DISTAL SETTING

S. No.	Ag	As	Au	Ba	Bi	Cu	Mn	Pb	Sb	Zn
P8N24	N0.025	73	0.002	1100	N1	16	29000	N1.0	N1	56
P8N26	N0.025	10	L0.002	42	N1	39	5800	1100.0	N1	710
P8N27	N0.025	53	N0.002	98	N1	31	240	9.2	N1	51
P8N28	N0.025	49	N0.002	56	N1	34	770	20.0	N1	130
P8N29	N0.025	580	N0.002	81	N1	310	24000	N1.0	N1	800
P8N30	N0.025	220	N0.002	11	N1	110	1100	190.0	N1	90
P8N31	N0.025	300	L0.002	16	N1	180	7900	820.0	N1	370
P8N32	N0.025	180	N0.002	31	N1	140	4000	20.0	N1	130
P8AL1	N0.025	110	L0.002	480	N1	660	3800	130.0	98	250
P8AL2	N0.025	23	0.050	8	N1	410	2400	23.0	N1	260

10. CHEMICAL SEDIMENTS (EXHALITES)—PROXIMAL SETTING

S. No.	Ag	As	Au	Ba	Bi	Cu	Mn	Pb	Sb	Zn
P8N01	N0.025	16.0	N0.002	1300	7.5	26.0	900	180.0	N1.0	81.0
P8N03	N0.025	34.0	N0.002	1300	N1.0	0.5	850	89.0	N1.0	15.0
P8N04	N0.025	4.4	N0.002	200	N1.0	16.0	720	140.0	N1.0	27.0
P8N05	N0.025	16.0	N0.002	1200	8.6	66.0	150	650.0	N1.0	120.0
P8N06	N0.025	N1.0	N0.002	1300	N1.0	11.0	51	1900.0	N1.0	17.0
P8N07	N0.025	N1.0	0.002	1300	N1.0	22.0	20	64.0	N1.0	11.0
P8N08	N0.025	7.3	N0.002	1300	N1.0	10.0	31	260.0	N1.0	24.0
P8N09	N0.025	17.0	N0.002	170	N1.0	17.0	190	220.0	N1.0	680.0
P8N10	N0.025	16.0	N0.002	1300	8.3	7.4	210	170.0	N1.0	6.6
P8N11	N0.025	5.3	N0.002	1300	7.4	41.0	170	220.0	N1.0	100.0
P8N12	4.800	75.0	N0.002	890	8.4	450.0	94	2600.0	64.0	1100.0
P8N13	1.300	9.9	0.002	920	9.0	130.0	37	32.0	37.0	13.0
P8N14	0.630	5.0	N0.002	400	8.7	430.0	92	17.0	N1.0	42.0
P8N15	0.870	13.0	N0.002	1300	12.0	180.0	12	150.0	10.0	34.0
P8N17	1.100	4.7	N0.002	990	13.0	31.0	32	29.0	6.0	11.0
P8N18	1.400	8.6	N0.002	230	12.0	260.0	66	170.0	7.6	41.0
P8N19	1.400	11.0	N0.002	350	12.0	100.0	45	96.0	74.0	30.0
P8N20	1.300	10.0	N0.002	1300	15.0	170.0	80	290.0	7.7	54.0
P8N21	N0.025	7.0	N0.002	320	12.0	4.1	94	29.0	N1.0	15.0
P8N22	N0.025	120.0	N0.002	4000	19.0	500.0	23	420.0	N1.0	270.0
P8N23	N0.025	1.0	N0.002	960	N1.0	6.1	96	19.0	N1.0	28.0
P8N33	N0.025	8.9	N0.002	250	N1.0	10.0	79	16.0	N1.0	17.0
P8N34	N0.025	7.7	N0.002	1200	N1.0	7.0	67	59.0	N1.0	17.0
P8N35	N0.025	6.0	N0.002	85	N1.0	2.0	35	6.7	N1.0	11.0
P8N36	N0.025	41.0	N0.002	120	N1.0	43.0	230	190.0	N1.0	500.0
P8N37	N0.025	5.1	N0.002	380	N1.0	1000.0	87	150.0	N1.0	88.0
P8N38	N0.025	5.3	N0.002	1300	N1.0	4.5	100	7.8	N1.0	7.9

11. MOMBEJA AREA—SERPENTINITE

Sample No.	Co	Cr	Cu	Ni	Zn
MBJ02B	11	14	59	29	27
MBJ03	60	110	65	670	27
MBJ04	85	260	65	1500	44
MBJ06	58	150	97	600	32
MBJ12	57	120	30	720	31

MBJ17	56	99	26	820	27
MBJ18	84	110	20	1700	31
MBJ20	85	190	35	1700	32
MBJ21	16	180	18	240	7
MBJ23	69	140	11	1300	31
MBJ29	42	210	41	830	10
MBJ33	62	140	21	1100	26
MBJ34B	21	210	73	300	6
MBJ38	63	410	150	880	25
MBJ40	46	230	55	1200	23
MBJ42	52	210	20	940	20
MBJ44	54	85	57	600	22
MBJ46	57	18	41	790	19
MBJ48	69	190	77	1000	31
MBJ49	68	310	40	1000	24
MBJ50	48	240	25	370	31
MBJ51	49	180	55	610	24
MBJ52	58	190	25	930	20

12. MOMBEJA AREA—LISTWAENITES

Sample No.	Co	Cr	Cu	Ni	Zn
MJB01	37.0	380	44.0	880	9
MJB02A	35.0	220	17.0	620	6
MJB05	12.0	120	16.0	160	14
MJB07	13.0	1	53.0	32	27
MJB08	5.9	26	83.0	18	9
MJB09	7.6	32	29.0	31	18
MJB10	6.3	35	5.6	29	14
MJB11	13.0	19	1.1	49	28
MJB13	29.0	320	26.0	400	52
MJB14	24.0	340	6.6	440	18
MJB15	37.0	410	6.9	830	10
MJB16	12.0	330	14.0	160	21
MJB19	28.0	210	15.0	310	11
MJB22	48.0	81	130.0	530	9
MJB24	35.0	240	18.0	750	10
MJB25	43.0	210	40.0	660	20
MBJ26	52.0	180	18.0	1200	10
MJB27	18.0	42	45.0	55	21
MJB28	11.0	58	14.0	36	23
MJB30	26.0	190	1.0	780	8
MJB31	43.0	180	18.0	590	10
MJB32	4.2	81	4.9	47	1
MJB34	16.0	240	18.0	240	7
MJB35	10.0	180	19.0	130	11
MJB36	24.0	42	2.1	43	24
MJB37	15.0	58	2.4	31	14
MJB39	30.0	130	3.8	570	9
MJB41	29.0	45	1.4	680	5
MJB43	27.0	180	25.0	550	15
MJB45	44.0	270	3.7	940	11
MJB47	45.0	19	16.0	920	13

13. SERRA BRANCA AREA—OUTCROPS AND DRILL CORE SAMPLES

Sample No.	Ag	As	Au	Cu	Mo	Pb	Zn
P8SB01	N0.025	11.0	N0.002	2.4	N1.0	6.6	43
P8SB02	N0.025	30.0	N0.002	N1.0	N1.0	17.0	40
P8SB03	N0.025	8.2	N0.002	2.2	N1.0	15.0	91
P8SB04	N0.025	N1.0	N0.002	380.0	N1.0	190.0	71
P8SB05	N0.025	4.1	N0.002	2.3	N1.0	35.0	71
P8SB06	N0.025	8.1	N0.002	1.3	N1.0	6.6	64
P8SB07	N0.025	9.9	N0.002	N1.0	N1.0	6.3	36
P8SB09	N0.025	220.0	N0.002	3.6	N1.0	5.9	54
P8SB10	N0.025	4.3	N0.002	1.9	N1.0	7.1	26
P8SB11	N0.025	N1.0	N0.002	4.2	N1.0	11.0	9
P8SB12	N0.025	N1.0	N0.002	2.5	N1.0	11.0	5
P8SB13	N0.025	N1.0	N0.002	2.0	N1.0	N1.0	1
P8SB14	N0.025	N1.0	N0.002	2.3	N1.0	6.2	18
P8SB15	N0.025	3.2	N0.002	2.6	N1.0	7.4	8
P8SB16	N0.025	3.4	N0.002	2.7	N1.0	11.0	25
P8SB17	N0.025	4.2	0.004	2.5	N1.0	8.3	20
P8SB18	0.520	N1.0	N0.002	2.2	N1.0	N1.0	5
P8SB19	0.490	N1.0	N0.002	1.3	N1.0	N1.0	7
P8SB20	N0.025	3.2	N0.002	1.5	N1.0	7.2	12
P8SB20	N0.025	4.4	N0.002	5.0	N1.0	14.0	23
P8SB21	N0.025	3.7	N0.002	91.0	N1.0	11.0	10
P8SB22	N0.025	3.3	N0.002	1.6	N1.0	5.7	37
P8SB23	N0.025	4.6	N0.002	18.0	N1.0	11.0	36
P8SB24	N0.025	N1.0	N0.002	5.6	N1.0	11.0	66
P8SB25	N0.025	N1.0	N0.002	130.0	4.0	N1.0	15
P8SB26	N0.025	27.0	N0.002	29.0	N1.0	24.0	30
P8SB27	N0.025	6.1	N0.002	2.8	N1.0	5.1	12
P8SB28	N0.025	N1.0	N0.002	2.8	N1.0	N1.0	3
P8SB29	N0.025	N1.0	N0.002	1.6	N1.0	N1.0	5
P8SB30	N0.025	N1.0	N0.002	2.8	N1.0	N1.0	4
P8SB32	N0.025	34.0	N0.002	1.0	4.8	N1.0	6
P8SB33	N0.025	37.0	N0.002	14.0	4.1	N1.0	10
P8SB34	N0.025	14.0	L0.002	9.5	13.0	6.8	6
P8SB35	N0.025	33.0	N0.002	3.4	3.5	N1.0	5
P8SB36	N0.025	8.4	N0.002	2.6	N1.0	N1.0	3
P8SB37	N0.025	9.1	N0.002	2.7	1.7	N1.0	3
P8SB38	N0.025	N1.0	N0.002	3.0	N1.0	N1.0	16
SB0701	N0.025	N1.0	N0.002	29.0	N1.0	9.2	63
SB0702	N0.025	N1.0	N0.002	15.0	N1.0	N1.0	18
SB0703	N0.025	N1.0	N0.002	17.0	N1.0	8.2	62
SB0704	N0.025	N1.0	N0.002	11.0	N1.0	12.0	37
SB0705	N0.025	N1.0	N0.002	11.0	N1.0	20.0	48
SB0706	N0.025	N1.0	N0.002	12.0	N1.0	11.0	51
SB0707	N0.025	N1.0	L0.002	57.0	N1.0	6.6	60
SB0708	N0.025	51.0	0.020	80.0	N1.0	28.0	19
SB0708A	N0.025	42.0	0.010	66.0	N1.0	10.0	17
SB0709	N0.025	N1.0	L0.002	2.6	N1.0	8.1	40
SB0710	N0.025	3.0	N0.002	15.0	N1.0	33.0	66

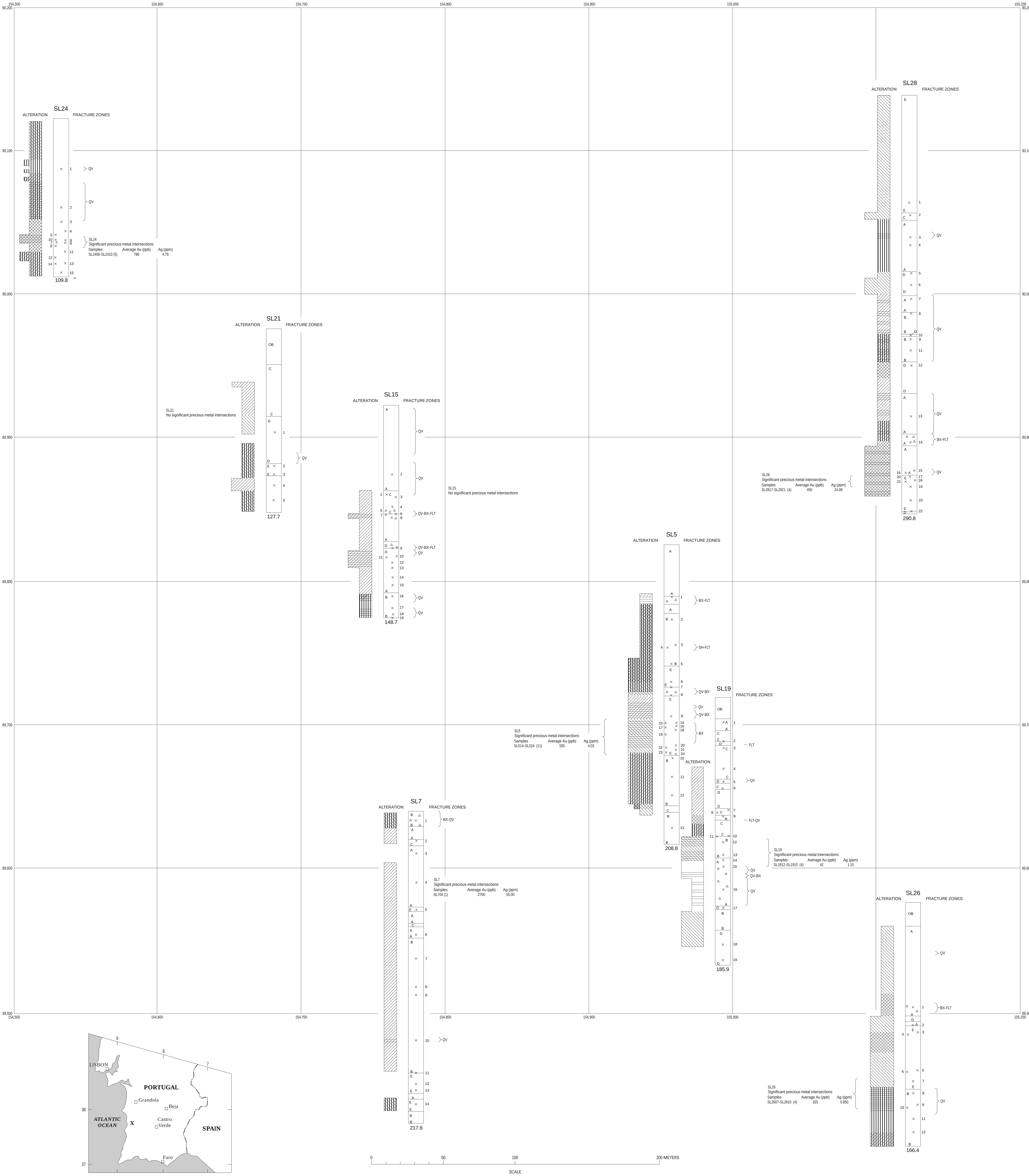

INDEX MAP OF SOUTHERN PORTUGAL SHOWING THE LOCATION OF THE SALGADINHO AREA (X)

EXPLANATION

Tops of drill log column represent location of drill hole collar. Coordinates from National Grid System (in meters)

Lithologic units

A **Argillaceous and partly carbonaceous shale and interlaminated siltstone, includes narrow intervals of phyllite, commonly weakly pyritic. Contains sedimentary slump structures and deformed bedding locally**

B **Laminated siliceous tuff, locally with interbeds of chloritic tuff and (or) lapilli tuff**

C **Phyllite, with quartz and sericite, light gray to light tan, locally contains interbeds of tuffite**

D **Tuffite, siliceous, fine grained, well sorted, locally with minor pyrite, thin to thick bedded and massive**

E **Felsic tuff, medium to coarse grained, porphyritic with quartz or quartz plus albite phenocrysts**

Structural features

QV **Quartz veins, locally contains carbonate minerals, pyrite and locally other sulfide minerals**

BX **Breccia formed primarily in or near fault zones, commonly contains quartz and ankerite in matrix**

SH **Shear zones, locally sericitic and chloritic, locally contains sulfide minerals**

FLT **Fault or fault zone**

Alteration

Ankerite, strong
Ankerite, moderate
Chlorite, strong
Chlorite, moderate
Sericite, strong
Sericite, moderate
Silica, consists of intense quartz veining or silica flooding

Sample localities

× 2 **Sample No. and number of samples collected**

△ **Breccia**

OB **Overburden**

DRILL HOLE DATA FROM THE SALGADINHO AREA, PORTUGAL

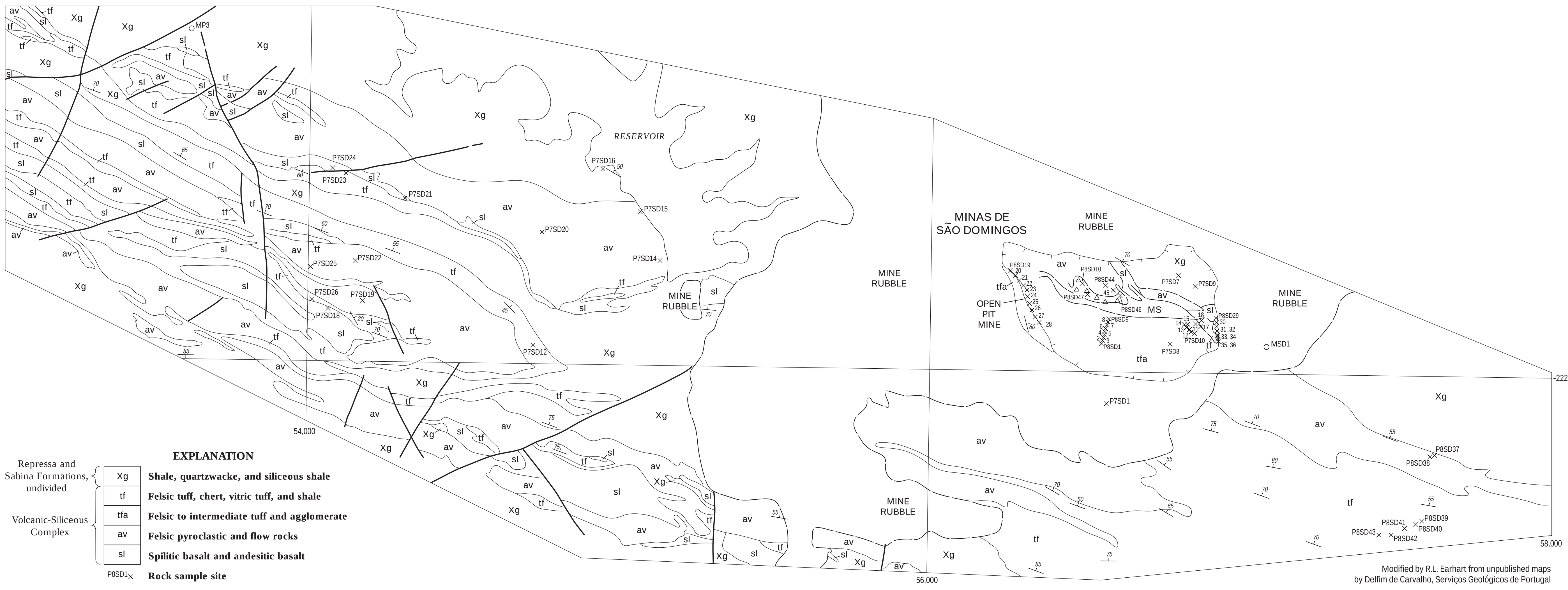

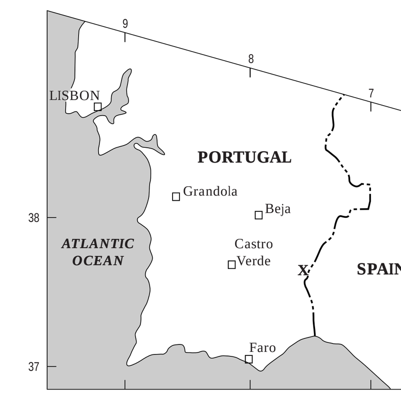

INDEX MAP OF SOUTHERN PORTUGAL SHOWING THE LOCATION OF THE SÃO DOMINGOS AREA (X)

EXPLANATION

Repressa and Sabina Formations, undivided

- Xg — **Shale, quartzwacke, and siliceous shale**

Volcanic-Siliceous Complex

- tf — **Felsic tuff, chert, vitric tuff, and shale**
- tfa — **Felsic to intermediate tuff and agglomerate**
- av — **Felsic pyroclastic and flow rocks**
- sl — **Spilitic basalt and andesitic basalt**

- P8SD1× — **Rock sample site**
- MP3○ — **Drill hole site**
- **Contact**
- **Fault**
- 70 — **Strike and dip**
- **Outline of mine rubble**

SCALE 1:10,000

0 — 0.5 — 1 KILOMETER

MAP A.—GENERALIZED GEOLOGIC MAP OF THE SÃO DOMINGOS AREA SHOWING SAMPLE LOCALITIES, PORTUGAL

SCALE 1:5,000

0 — 0.5 — 1 KILOMETER

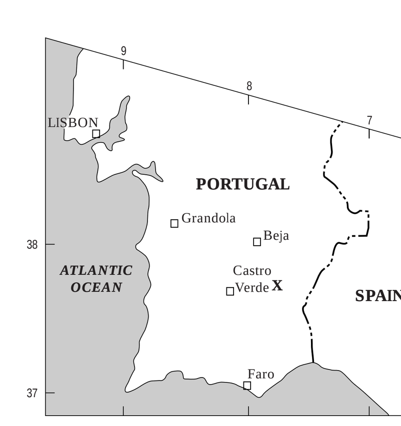

INDEX MAP OF SOUTHERN PORTUGAL SHOWING THE LOCATION OF THE SERRA BRANCA AREA (X)

EXPLANATION

- M — **Mértola Formation**
- bv — **Borra do vinho (purple shale)**
- vt — **Vitric tuff**
- j — **Jasper**
- sh — **Shale**
- ft — **Felsic tuff**
- taa — **Altered tuff and agglomerate**
- ag — **Agglomerate**
- tai — **Tuff and agglomerate, felsic to intermediate**
- ti — **Tuff, intermediate**
- rb — **Rhyolite flow**
- tf — **Tuffite**
- PQ — **Phyllite-Quartzite Group**—Pyrite (iron hydroxide rich) zones
- **Normal fault**—Queried where uncertain
- **Thrust fault**—Sawteeth on upper plate. Queried where uncertain
- 70 — **Strike and dip of beds**
- 70 — **Strike and dip of foliation**
- 77 — **Strike and dip of rock cleavage**
- P8SB6× — **Sample locality and number**
- SB7○ — **Drill hole and number**

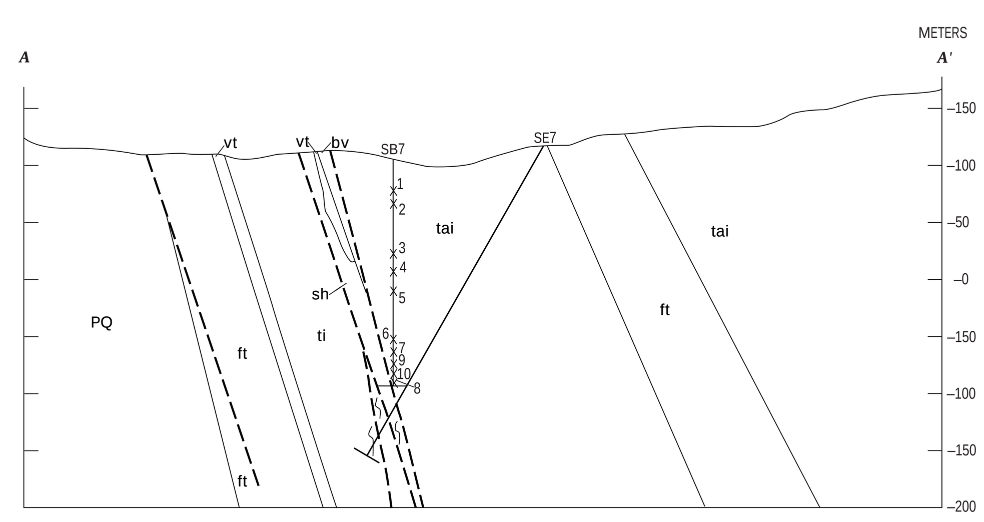

EXPLANATION

- tai — **Tuff, agglomeratic, felsic to intermediate**
- ft — **Tuff, intermediate**
- ti — **Tuff, felsic**
- bv — **Borra do Vinho purple shale**
- vt — **Vitric tuff**
- sh — **Black to green-gray shale**
- PQ — **Quartzite Group phyllite**
- **Fault**
- SB7 — **Drill hole**
- x1 — **Drill core sample and number**

Sample No.	Core sample descriptions
SB7-1	Calcite-quartz veinlet with rhodochrosite and vuggy pyrite, hosted in coarse agglomerate, 12 mm thick
SB7-2	Quartz vein, minor calcite, agglomerate inclusions, 32 cm thick
SB7-3	Andesitic agglomerate, chloritic, trace pyrite
SB7-4	Dacite-keratophyre, round quartz phenocrysts, disseminated pyrite
SB7-5	Same as SB7-4
SB7-6	Dacite-keratophyre, round quartz phenocrysts, trace pyrite
SB7-7	Dacite-keratophyre, very chloritic, minor pyrite
SB7-8	Highly silicified pyroclastic rock, 70 percent pyrite
SB7-9	Dacite-keratophyre, highly chloritic, albitic, calcite vugs, pyrite
SB7-10	Dacite-keratophyre, sheared, with calcite and pyrite

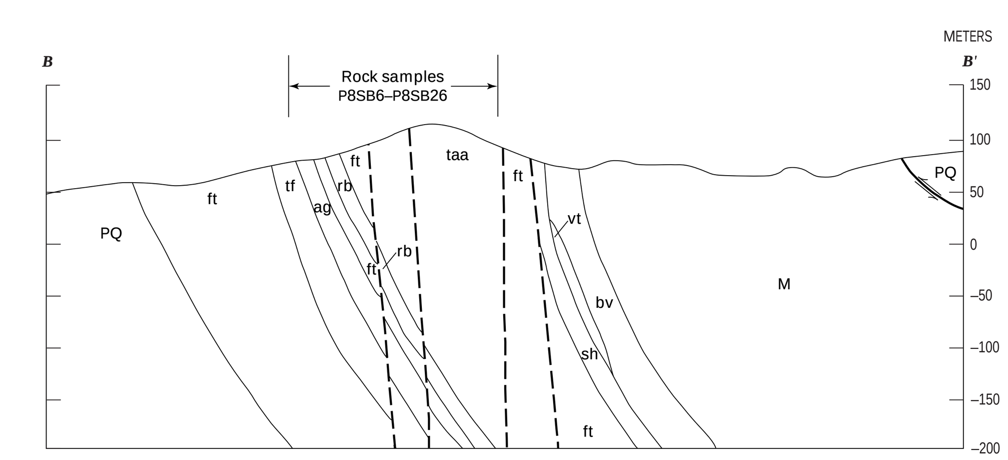

EXPLANATION

- M — **Mértola Formation**
- bv — **Borra do vinho (purple shale)**
- vt — **Vitric tuff**
- sh — **Shale**
- ft — **Felsic tuff**
- taa — **Altered tuff and agglomerate**
- rb — **Flow-banded rhyolite**
- ag — **Agglomerate**
- tf — **Tuffite**
- PQ — **Phyllite-Quartzite Group**
- **Contact**
- **Fault**—Arrows show direction of movement

DESCRIPTION

Sample No.	Core sample descriptions
P8SB6	Felsic tuff, argillically altered, sheared, greenish mica
P8SB7	Same as P8SB6
P8SB7	Same as P8SB6
P8SB8	Felsic tuff, sheared, greenish mica, Fe oxides minor chlorite
P8SB9	Same as P8SB9
P8SB10	Felsic tuff, with greenish mica, Fe oxides, in veinlets
P8SB11	Green-altered tuff, quartz phenocrysts, minor pyrite
P8SB12	Green-altered tuff, pink feldspar veinlets
P8SB13	Sub-vitreous tuff, quartz phenocrysts
P8SB14	Green-altered tuff, quartz and albite phenocrysts
P8SB15	Silicified green-altered tuff, chlorite stringers
P8SB16	Agglomerate, weakly silicified, weekly chloritic
P8SB17	Green-altered tuff
P8SB18	Banded vitric tuff, trace pyrite
P8SB19	Green-altered tuff, highly sheared
P8SB20	Felsite
P8SB21	Ferruginous quartz from fault zone
P8SB22	Quartz keratophyre
P8SB23	Sheared, ferruginous tuff from fault zone
P8SB24	Quartz keratophyre
P8SB25	Flow-banded rhyolite
P8SB26	Laminated tuffite
X	Sample locality
FLT	Fault or fault zone

MAP B.—GEOLOGIC MAP SHOWING SAMPLE LOCALITIES IN THE SERRA BRANCA AREA, PORTUGAL

USGS
science for a changing world